High temperature phase transition in two-scalar theories

S. Bornholdt*
Institut für Theoretische Physik, Universität Heidelberg, Philosophenweg 16, 69120 Heidelberg, Germany

N. Tetradis
Theoretical Physics, University of Oxford, 1 Keble Road, Oxford OX1 3NP, United Kingdom

C. Wetterich
Institut für Theoretische Physik, Universität Heidelberg, Philosophenweg 16, 69120 Heidelberg, Germany
(Received 5 June 1995)

Two-scalar theories at high temperature exhibit a rich spectrum of possible critical behavior, with a second or first order phase transition. In the vicinity of the critical temperature one can observe critical exponents, tricritical points, and crossover behavior. None of these phenomena are visible to high temperature perturbation theory.

PACS number(s): 11.10.Wx, 64.60.Ak, 64.60.Fr, 98.80.Cq

I. INTRODUCTION

Scalar field theories have been the prototype for investigations concerning the question of symmetry restoration at high temperature. Following the original argument of Kirzhnits and Linde [1], the O(N)-symmetric scalar theory was considered in subsequent studies of the problem [2–4]. The framework in which these studies were carried out is the perturbative evaluation of the effective potential [5] and its generalization for nonzero temperature. Even though the restoration of the spontaneously broken symmetry was qualitatively demonstrated, the investigation of the details of the phase transition was not possible, due to infrared divergences rendering the perturbative approach unreliable near the critical temperature [3,4]. These divergences originate in the absence of an infrared cutoff in higher loop contributions when the temperature-dependent mass of the scalar fluctuations approaches zero near the critical temperature. An amelioration of the situation was achieved through the summation of an infinite subclass of perturbative contributions (the ''daisy'' graphs) [2]. Indeed, these contributions become dominant for large N and a quantitative description of the phase transition can be obtained in this limit. However, the physical picture remained unclear for small, physically relevant values of N, for which even the order of the transition was not established. The question was resolved [6] through the method of the effective average action [7–10], which relies on the renormalization-group approach. The phase transition was shown to be second order for all values of N. The quantitative behavior near the critical temperature was studied in detail and the critical system was found to have an effectively three-dimensional character. Its behavior can be characterized by critical exponents [6,10], in agreement with known results from three-dimensional field theory. The picture was verified through an independent analysis in the large N limit [11], with use of other nonperturbative methods, such as the solution of the Schwinger-Dyson equations. A summary of the results can be found in Ref. [12].

In a cosmological context first-order phase transitions are more spectacular than second order transitions due to the departure from thermal equilibrium. One would like to have a prototype model for a first-order transition, for which the methods of high-temperature field theory can be tested, similar to the O(N) scalar model for second-order transitions. In statistical physics it is well known that scalar models with more than one field and discrete symmetries instead of maximal O(N) symmetry exhibit a rich spectrum of critical behavior, including first- and second-order transitions and tricritical behavior in between. Since high-temperature field theories are in close correspondence to (three-dimensional) statistical models, it seems natural to investigate such models also as prototypes for first order transitions in high-temperature field theory. In this paper we apply the method of the effective average action to the study of the high-temperature phase transitions in theories with two real scalar fields. The symmetry is not O(2), but rather a discrete symmetry. This model can serve as a prototype for a first-order phase transition in field theories. It can be easily generalized to models in which each scalar field is an N-component vector.

We are interested in the phenomenon of spontaneous symmetry breaking and symmetry restoration at high temperature. For sufficiently low temperature our two-scalar theory models the Higgs mechanism in gauge theories, through which the expectation value of a scalar field results in a mass term for gauge fields.[1] Perturbative arguments predict a first-order phase transition for this case [13]. However, the reliability of such predictions is questionable when the transition

*Present address: Institut für Theoretische Physik, Universität Kiel, Olshausenstr. 6, 24118 Kiel, Germany.

[1]For sufficiently small-gauge coupling the present investigation and its generalization to the case where each scalar field has N components gives a reasonable approximation to the gauged models even in the vicinity of the critical temperature. However, the determination of the meaning of ''sufficiently small'' needs a detailed investigation of high-temperature gauge theories.

becomes weakly first order, due to infrared divergences similar to the ones plaguing the study of the O(N)-symmetric scalar theory [14]. The approximate vanishing of some mass near the critical temperature results in the absence of an infrared cutoff in higher loop contributions of perturbation theory. In two-scalar theories this is connected with the fact that one of the fields gets its mass (or part of it) through the expectation value of the other.

The present work obtains control over these infrared problems.[2] Depending on the couplings of the model we find that the phase transition is either first or second order. For a sufficiently strongly first-order transition high-temperature perturbation theory may give realistic results for the two-scalar model. We concentrate here on the more problematic regions of a second-order transition, a weakly-first-order transition, and the tricritical behavior at the separation of the two regimes. For the corresponding values of the couplings high-temperature perturbation theory fails near the critical temperature. As a by-product, our results can be used in order to establish in which region of parameter-space perturbation theory gives a reasonable for the description of the phase transition.

Our results are relevant for two specific classes of scenarios in the cosmological context. The first class concerns multi-Higgs-scalar extensions of the standard model at nonzero temperature. The prediction of perturbation theory for a first-order electroweak phase transition [13], combined with the existence of baryon number violating processes at nonzero temperature within the standard model [18], has generated much interest in the probability of creating the baryon asymmetry of the universe during the electroweak phase transition. Several scenarios have been proposed [19] and the electroweak phase transition has been studied with a variety of methods [20]. (For an overview of the extensive literature see Ref. [21].) It is not clear, however, if the phase transition in the pure standard model is sufficiently strongly first order and if there is sufficient CP violation in order to create an asymmetry of reasonable size. This has led to the study of multi-Higgs-scalar extensions of the standard model, in which the additional scalar fields can be used to make the phase transition more strongly first order or to enhance the sources of CP violation in the model. Also supersymmetric extensions of the standard model contain two-scalar doublets. It is not clear whether the perturbative methods used in Ref. [22] for the calculation of the scalar field contributions to the effective potential are reliable for such two-scalar models, if we take into account the ''warning'' from the study of the O(N)-symmetric theory. Our work gives a reliable estimate of the effect of these contributions on the nature of the transition.

The second class of scenarios concerns multi-scalar models of inflation [23]. In most such studies some classical potential is employed, which may bear no resemblance to the effective potential. Thermal effects are often ignored except for the temperature dependence of the mass term. If inflation is initiated by a high-temperature phase transition our formalism sets the framework for the proper study of the problem.

We consider a theory of two real scalar fields $\chi_a (a=1,2)$, invariant under the discrete symmetries $(\chi_1 \leftrightarrow -\chi_1, \chi_2 \leftrightarrow -\chi_2, \chi_1 \leftrightarrow \chi_2)$, which we denote by $(1 \leftrightarrow -1,\ 2 \leftrightarrow -2,\ 1 \leftrightarrow 2)$ for brevity. The symmetry group is $Z_4 \times Z_2$, consisting of 90° rotations in the (χ_1, χ_2) plane and a reflection on one of the axes. The classical potential can be written as

$$V(\chi_1,\chi_2) = \frac{1}{2}\bar{m}^2(\chi_1^2+\chi_2^2+\chi_2^2) + \frac{1}{8}\bar{\lambda}(\chi_1^4+\chi_2^4) + \frac{1}{4}\bar{g}\chi_1^2\chi_2^2$$
$$= \frac{1}{2}\bar{m}^2(\chi_1^2+\chi_2^2) + \frac{1}{8}\bar{\lambda}(\chi_1^2+\chi_2^2)^2 + \frac{1}{4}x\bar{\lambda}\chi_1^2\chi_2^2, \tag{1.1}$$

with

$$x = \frac{\bar{g}}{\bar{\lambda}} - 1. \tag{1.2}$$

For V to be bounded from below we require $\bar{\lambda} > 0$, $x > -2$.

For $\bar{m}^2 > 0$ the classical theory is in the symmetric regime (which we denote by S) with the minimum of the classical potential at the origin. For $\bar{m}^2 < 0$ the theory is in the spontaneously broken regime and we distinguish two possibilities consistent with the symmetry.

(I) For $x < 0$ four degenerate minima of the potential are located between the two axes at

$$\chi_{10} = \pm\chi_{20} = \pm\sqrt{-2\bar{m}^2/(\bar{\lambda}+\bar{g})}. \tag{1.3}$$

We denote this regime by M.

(II) For $x > 0$ the four minima of the potential are located on the axes at

$$\chi_{10} = \pm\sqrt{-2\bar{m}^2/\bar{\lambda}}, \quad \chi_{20} = 0, \tag{1.4}$$

or similarly with χ_{10} and χ_{20} interchanged. We denote this regime by AX. The regimes M and AX are closely related. A redefinition of the fields according to

$$\tilde{\chi}_1 = \frac{1}{\sqrt{2}}(\chi_1+\chi_2), \quad \tilde{\chi}_2 = \frac{1}{\sqrt{2}}(\chi_1-\chi_2) \tag{1.5}$$

results in a rotation of the axes by 45°, thus transforming the AX into the M regime. The couplings of the redefined theory are related to the old ones according to

$$\tilde{\lambda} = \bar{\lambda}\left(1+\frac{x}{2}\right), \quad \tilde{x} = -\frac{x}{1+\frac{x}{2}}. \tag{1.6}$$

There are three characteristic values of x: (a) For $x=0$ the symmetry of the theory is increased to O(2); (b) for $x=-1$

[2] We should point out that, for a non-Abelian Higgs model, the situation is much more involved than the perturbative results indicate, due to the presence of a confining regime in the symmetric phase of the model. As this work deals only with scalar fields, such a complication does not arise. For a discussion of gauge theories in the context of the effective average action approach see Refs. [15–17].

the theory decomposes into two disconnected Z_2-symmetric models for χ_1 and χ_2 separately; (c) similarly, for $x=2$ [and therefore $\tilde{x}=-1$, according to Eq. (1.6)] the theory decomposes into two disconnected Z_2-symmetric models for $\tilde{\chi}_1$ and $\tilde{\chi}_2$. The above symmetries are expected to be preserved after the quantum or thermal corrections have been taken into account. This means that any renormalization-group flow of the couplings that starts on the surfaces $x=0,-1,2$ in parameter space cannot take the system out of them. As a result the parameter space of the theory is divided into the four regions $x>2$, $2>x>0$, $0>x>-1$, $x<-1$, which are not connected by the renormalization-group flow of the couplings. The phase transitions for the theories which correspond to $x=0,-1,2$ have been discussed in detail in Refs. [6,10]. They are second-order transitions governed by effectively three-dimensional fixed points. In our model these fixed points exist on surfaces separating the parameter space into disconnected regions. We shall demonstrate all the above points in the following sections.

We should point out that this model was discussed in Ref. [24] through use of finite-temperature perturbation theory. No part of the rich structure of critical behavior that we shall describe in the following sections was observed. The universal, effectively three-dimensional behavior of the system near the critical temperature is common for statistical systems and three-dimensional field theories which belong to the same universality class. (The statistical systems are characterized as two-component spin systems with cubic anisotropy.) As a consequence, various aspects of the problem have been investigated in Refs. [25–28] (and references therein) through other methods. Our results are in very good agreement with all these studies. Similar models have been considered in Ref. [29].

The outline of our procedure follows. We make use of the effective average action Γ_k, which results from the effective integration of quantum and thermal fluctuations with characteristic momenta $q^2>k^2$. It contains all the information on the generalized couplings of the theory and their dependence on the scale k. For k of the order of some ultraviolet cutoff Λ the effective average action is equal to the classical (bare) action (no integration of fluctuations takes place). For $k=0$, Γ_k is equal to the effective action (all fluctuations are integrated). The dependence of Γ_k on the scale k is given by an exact nonperturbative renormalization-group equation, which can be expressed as evolution equations for the running couplings of the theory. These equations can be solved within some appropriate approximation scheme, with the classical couplings as initial conditions for $k=\Lambda$. The renormalized couplings of the theory are obtained for $k=0$. The calculation can be performed for zero and nonzero temperature. The gradual incorporation of the effects of quantum and thermal fluctuations into the running couplings is the essential element which resolves the problem of infrared divergences that invalidates perturbative schemes. The basic formalism of the effective average action is summarized in Sec. II. We expect that the running of the couplings for k much smaller than the temperature has an effectively three-dimensional character. The reason is that the effective dimensionality is reduced, when the characteristic length scale $1/k$ of the ''coarse-grained'' system is much larger than the periodicity $1/T$ in the imaginary time direction set by the temperature. This is expected to be important near the critical temperature, where no infrared cutoffs (such as masses) other than k exist. As a result, the fixed-point structure of the three-dimensional theory determines the behavior of the critical system. For this reason we present in Sec. III a qualitative study of the three-dimensional theory and its fixed points, based on a crude approximation scheme for the solution of the exact renormalization-group equation. In Sec. IV, we develop more elaborate (and, therefore, more accurate) approximation schemes. They are generalized for nonzero temperature in Sec. V. These tools are put into work in Secs. VI and VII: The evolution of the running couplings is calculated, starting with the classical theory at scales $k=\Lambda\gg T$ and finishing at $k=0$, where the renormalized theory is obtained. In Sec. VII we explicitly demonstrate how the evolution of the running couplings becomes effectively three dimensional for $k\ll T$. In Sec. VIII we calculate the critical temperature for the phase transition. In Secs. IX–XI we discuss the details of this transition. We observe a rich spectrum of critical behavior with critical exponents, crossover phenomena, tricritical points, etc. None of these are visible within perturbation theory. Our conclusions are given in Sec. XII.

II. THE EVOLUTION EQUATION FOR THE EFFECTIVE AVERAGE POTENTIAL

We consider a theory of two real scalar fields χ_a $(a=1,2)$, in d-dimensional Euclidean space, with an action $S[\chi]$ invariant under the $(1\leftrightarrow-1,\ 2\leftrightarrow-2,\ 1\leftrightarrow2)$ symmetry. We specify the action together with some ultraviolet cutoff Λ, so that the theory is properly regulated. We add to the kinetic term an infrared regulating piece [9]

$$\Delta S=\frac{1}{2}\int\frac{d^dq}{(2\pi)^d}R_k(q)\chi_a^*(q)\chi^a(q), \tag{2.1}$$

where $\chi^a(q)$ are the Fourier modes of the scalar fields. The function R_k is employed in order to prevent the propagation of modes with characteristic momenta $q^2<k^2$. This can be achieved, for example, by the choice

$$R_k(q)=\frac{q^2f_k^2(q)}{1-f_k^2(q)}, \tag{2.2}$$

with

$$f_k^2(q)=\exp\left(-\frac{q^2}{k^2}\right). \tag{2.3}$$

We point out that there are many alternative choices for $R_k(q)$, some of which were used in Refs. [7–12]. The physical results which are obtained when the cutoff is removed are scheme independent. The choice of Eqs.(2.2), (2.3) is the most natural one [9] and is convenient for numerical calculations. For a massless field the inverse propagator derived from the action $S+\Delta S$ has a minimum $\sim k^2$. The modes with $q^2\gg k^2$ are unaffected by the infrared cutoff, while the low frequency modes with $q^2\ll k^2$ are cut off, as R_k acts like a mass term

$$\lim_{q^2\to0}R_k(q)=k^2. \tag{2.4}$$

We subsequently introduce sources and define the generating functional for the connected Green functions for the action $S+\Delta S$. Through a Legendre transformation we obtain the generating functional for the one particle irreducible (1PI) Green functions $\tilde{\Gamma}_k[\phi^a]$, where ϕ^a is the expectation value of the field χ^a in the presence of sources. The use of the modified propagator for the calculation of $\tilde{\Gamma}_k$ results in the effective integration of only the fluctuations with $q^2>k^2$. Finally, the effective average action is obtained by removing the infrared cutoff:

$$\Gamma_k[\phi^a]=\tilde{\Gamma}_k[\phi^a]-\frac{1}{2}\int\frac{d^dq}{(2\pi)^d}R_k(q)\phi_a^*(q)\phi^a(q). \tag{2.5}$$

For k equal to the ultraviolet cutoff Λ, Γ_k becomes equal to the classical action S (no effective integration of modes takes place), while for $k\to 0$ it tends towards the effective action Γ (all the modes are included) which is the generating functional of the 1PI Green functions computed from S (without infrared cutoff). For intermediate values of k the effective average action realizes the concept of a coarse-grained effective action in the sense of Ref. [30].

The interpolation of Γ_k between the classical and the effective action makes it a very useful field theoretical tool. The means for practical calculations is provided by an exact flow equation[3] which describes the response of the effective average action to variations of the infrared cutoff $[t=\ln(k/\Lambda)]$ [9]:

$$\frac{\partial}{\partial t}\Gamma_k[\phi]=\frac{1}{2}\mathrm{Tr}\left([\Gamma_k^{(2)}(\phi)+R_k]^{-1}\frac{\partial}{\partial t}R_k\right). \tag{2.6}$$

Here $\Gamma_k^{(2)}$ is the second functional derivative of the effective average action with respect to ϕ^a. For real fields it reads, in momentum space,

$$(\Gamma_k^{(2)})_b^a(q,q')=\frac{\delta^2\Gamma_k}{\delta\phi_a^*(q)\,\delta\phi^b(q')}, \tag{2.7}$$

with

$$\phi^a(-q)=\phi_a^*(q). \tag{2.8}$$

The nonperturbative flow equation has the form of a one-loop expression involving the exact inverse propagator $\Gamma_k^{(2)}$ together with an infrared cutoff provided by R_k. No contributions from higher loops appear in this exact equation.

For the solution of Eq. (2.6) one has to develop an efficient truncation scheme. The form of the effective average action is constrained by the $(1\leftrightarrow -1,\ 2\leftrightarrow -2,\ 1\leftrightarrow 2)$ symmetry. However, there is still an infinite number of invariants to be considered. Throughout this paper we shall work with an approximation which neglects the effects of wave-function renormalization. We shall, therefore, keep only a classical kinetic term in the effective average action

$$\Gamma_k=\int d^dx\left\{U_k(\rho_1,\rho_2)+\frac{1}{2}\partial^\mu\phi_a\partial_\mu\phi^a\right\}, \tag{2.9}$$

and neglect all invariants which involve more derivatives of the fields. We have used the definition $\rho_1=\frac{1}{2}\phi_1^2$ and similarly for ρ_2. The justification for our approximation lies in the smallness of the anomalous dimension, which is expected to be $\eta\simeq 0.03-0.04$ for the three-dimensional theory. We estimate the corrections arising from the proper inclusion of wave-function renormalization effects to be of the same order as η (a few percent). An improved treatment will be given elsewhere [36]. In order to obtain an evolution equation for U_k from Eq. (2.6), we have to expand around a constant field configuration [so that the derivative terms in the parametrization (2.9) do not contribute to the left-hand side (LHS) of Eq. (2.6)]. Equation (2.6) then gives [8–10]

$$\frac{\partial}{\partial t}U_k(\rho_1,\rho_2)=\frac{1}{2}\int\frac{d^dq}{(2\pi)^d}\left(\frac{1}{P(q^2)+M_1^2}+\frac{1}{P(q^2)+M_2^2}\right)\frac{\partial}{\partial t}R_k(q). \tag{2.10}$$

$P(q^2)$ results from the combination of the classical kinetic contribution q^2 and the regulating term R_k into an effective inverse propagator (for massless fields)

$$P(q^2)=q^2+R_k=\frac{q^2}{1-f_k^2(q)}, \tag{2.11}$$

with $f_k^2(q)$ given by Eq. (2.3). For $q^2\gg k^2$ the inverse "average" propagator $P(q)$ approaches the standard inverse propagator q^2 exponentially fast, whereas for $q^2\ll k^2$ the infrared cutoff prevents the propagation. $M_{1,2}^2$ are the eigenvalues of the mass matrix at the point (ρ_1,ρ_2),

$$M_{1,2}^2(\rho_1,\rho_2)=\frac{1}{2}\{U_1+U_2+2U_{11}\rho_1+2U_{22}\rho_2\pm[(U_1-U_2+2U_{11}\rho_1-2U_{22}\rho_2)^2+16U_{12}^2\rho_1\rho_2]^{1/2}\}, \tag{2.12}$$

and we have introduced the notation $U_1=\partial U_k/\partial\rho_1$, $U_{12}=\partial^2U_k/\partial\rho_1\partial\rho_2$, etc.

Equation (2.10) is the master equation for our investigation. It is a nonlinear partial differential equation for three independent variables $(t,\ \rho_1,\ \rho_2)$. Since it is difficult to solve it exactly we again resort to some approximation scheme. We first introduce a Taylor expansion of $U_k(\rho_1,\rho_2)$ around its minimum. This turns Eq. (2.10) into an infinite system of ordinary (coupled) differential equations for the k dependence of the minimum and the derivatives of the effective average potential, with independent variable $t=\ln(k/\Lambda)$. We solve this system approximately by truncating at a finite number of derivatives. This approach has been used in the past for the study of the O(N)-symmetric scalar theory. It has provided a full, detailed picture of the high-temperature phase transition for this theory [6,10–12], with accurate determination (at the few percent level) of such nontrivial quantities as the critical exponents [10]. An esti-

[3]See Ref. [31] for other versions of exact renormalization-group equations.

mate [32] of the residual errors for high level truncations indicates that they are smaller than the uncertainties introduced by the imprecise treatment of the wave-function renormalization effects. For this work we shall use the lowest-level truncation, which keeps only the second derivatives of the potential U_{11}, U_{22}, U_{12}. This will be sufficient for a reliable determination of the phase diagram and a crude estimate of universal quantities such as critical exponents and crossover curves. For an improved treatment see Ref. [35], and for a discussion which takes into account the next level in the truncation for U_k and the first corrections arising from wave-function renormalization see Ref. [36].

III. THE PHASE STRUCTURE OF THE THREE-DIMENSIONAL THEORY

Before performing a more detailed analysis we would like to gain some understanding of the phase structure of the theory. As we have already mentioned in the introduction, the behavior of the four-dimensional theory near a high-temperature second-order phase transition is expected to have a three-dimensional character. The reason for this is the divergence of the correlation length for the fluctuations of the system (the mass of some fields goes to zero). As a result, the characteristic length scale for the critical system is much larger than the periodicity in the imaginary time direction due to temperature[4] (for details see the following sections). This leads to dimensional reduction and the critical system has effectively three-dimensional behavior. For this reason we are interested in the phase structure of the three-dimensional theory. More specifically we want to investigate the possible existence of fixed points which govern the dynamics of second-order phase transitions.

For the purpose of this section we parametrize the potential by its derivatives at the origin (S regime):

$$\bar{m}^2(k)=U_1(0)=U_2(0), \quad \bar{\lambda}(k)=U_{11}(0)=U_{22}(0),$$

$$\bar{g}(k)=U_{12}(0), \quad x(k)=\frac{\bar{g}(k)}{\bar{\lambda}(k)}-1. \tag{3.1}$$

The equality of U_1, U_2 and U_{11}, U_{22} is imposed by the $(1\leftrightarrow -1,\ 2\leftrightarrow -2,\ 1\leftrightarrow 2)$ symmetry of the theory. For the potential to be bounded we also require $x>-2$. For a rough estimate the three-dimensional couplings are related to the effective couplings of the four-dimensional theory at high temperature by $\bar{\lambda}(2\pi T)=\lambda_4 T, \bar{g}(2\pi T)=g_4 T$, $\bar{m}^2(2\pi T)=m_4^2+cT^2$, with appropriate c (for details see Secs. VI and VII). Evolution equations for the above parameters are obtained by taking derivatives of Eq. (2.10) with respect to $\rho_{1,2}$. It is convenient to define the dimensionless couplings

$$m^2(k)=\frac{\bar{m}^2(k)}{k^2}, \quad \lambda(k)=\frac{\bar{\lambda}(k)}{k}, \quad g(k)=\frac{\bar{g}(k)}{k}. \tag{3.2}$$

In terms of these quantities the evolution equations have a scale-invariant form, in the sense that the RHS does not explicitly involve a dependence on k:

$$\frac{dm^2}{dt}=-2m^2+v_3(4+x)\lambda L_1^3(m^2), \tag{3.3}$$

$$\frac{d\lambda}{dt}=-\lambda-v_3(10+2x+x^2)\lambda^2 L_2^3(m^2), \tag{3.4}$$

$$\frac{dx}{dt}=v_3(x+1)x(x-2)\lambda L_2^3(m^2), \tag{3.5}$$

where $v_3=1/8\pi^2$. The threshold functions $L_n^3(w)$ suppress the contributions of massive modes to the evolution equations. They are studied in detail in the following sections.

We are interested in the fixed points of the last set of equations. For any x, there is an ultraviolet-attractive Gaussian fixed point with $m^2=\lambda=0$. There are also three fixed points with at least one infrared attractive direction [25–28]. They all appear for $m^2<0$, $\lambda>0$. (The exact values are not important since the discussion in this section is only qualitatively correct.) For their identification we use their standard names in statistical physics [25,27]. (a) The Heisenberg fixed point has $x=0$ and corresponds to a theory with symmetry increased to O(2), as we have discussed in the introduction. (b) The Ising fixed point has $x=-1$ and corresponds to two disconnected Z_2-symmetric theories. (c) The cubic fixed point has $x=2$ and corresponds to two disconnected theories, if the fields are redefined according to Eq. (1.5). All these points are infrared unstable in the m^2 direction and are located on a critical surface $m_{\rm cr}^2=m_{\rm cr}^2(\lambda,x)<0$. Solutions of the evolution equations which start above the critical surface, with $m^2>m_{\rm cr}^2$, flow towards the region of positive m^2 for $t\to-\infty$, and correspond to theories in the symmetric phase. Solutions with $m^2<m_{\rm cr}^2$ flow deep into the region of negative m^2 and correspond to theories in the phase with spontaneous symmetry breaking.

The relative stability of the fixed points on the critical surface determines which one governs the dynamics of the phase transition very close to the critical temperature. For a first simple investigation of the relative stability in the (λ,x) directions we fix m^2 to an arbitrary value (we choose $m^2=0$ for convenience) and solve Eqs. (3.4), (3.5) numerically. The results are presented in Fig. 1. We observe that all three fixed points are attractive in the λ direction. However, the Ising and cubic fixed points are repulsive in the x direction, while the Heisenberg fixed point is totally attractive. We observe four disconnected regions.

(a) $2>x>0$. The trajectories flow away from the cubic and towards the Heisenberg fixed point.

(b) $0>x>-1$. The trajectories flow away from the Ising and towards the Heisenberg fixed point.

(c) $x>2$. The trajectories flow away from the cubic fixed point and into a region of large x and small λ. Eventually λ turns negative at a finite value of k. [This can be verified through the explicit solution of Eqs. (3.4), (3.5) in this region.] At this point an instability arises, as the potential seems not to be bounded from below. Our treatment is not sufficient for a detailed investigation of the nature of this

[4] If the phase transition is strongly first order this need not be true, because the mass of the fluctuations does not go to zero and the correlation length does not diverge near the transition.

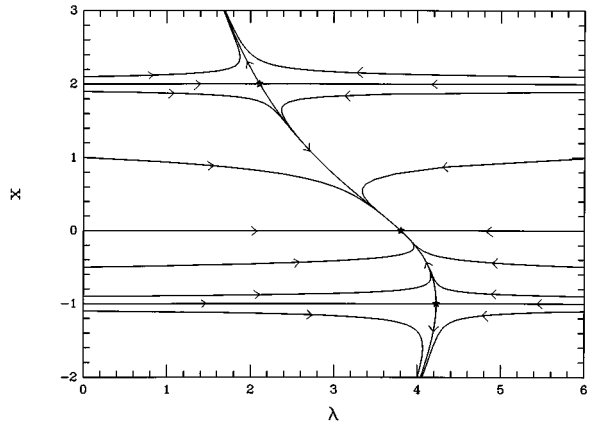

FIG. 1. Flows on the (λ,x) plane for the three-dimensional theory. The evolution is determined by Eqs. (3.4), (3.5) with $m^2=0$.

instability, since our truncation scheme is very crude. A detailed discussion is given in Ref. [35], where improved truncations are employed. It is shown that the instability is not real since the higher derivatives of the potential remain positive. The change of sign for λ corresponds to the disappearance of a false vacuum of the theory and results in a first-order phase transition. We shall return to this point in the following sections.

(d) $x<-1$. The trajectories flow away from the Ising fixed point and cross the line $x=-2$ at a finite k. This again implies the presence of an instability whose true nature is related to the disappearance of a false vacuum. The model exhibits a first-order transition also for $x<-1$. Flows that start on the lines $x=0$, -1, 2 remain on these lines. No trajectories exist which connect the four regions $x>2$, $2>x>0$, $0>x>-1$, $x<-1$. All this is in agreement with the discussion at the end of the introduction.

The diagram of Fig. 1 determines the phase structure of the theory when the behavior of the system becomes effectively three-dimensional (i.e., close to the critical temperature). For parameters in the regions $2>x>0$, $0>x>-1$ we expect second-order phase transitions, with critical dynamics governed by the three fixed points. These two regions can be mapped onto each other through a redefinition of the fields according to Eqs. (1.5) and (1.6). This indicates that the Ising and cubic fixed points should lead to identical universal behavior (and therefore to identical universal quantities, such as critical exponents). Very close to the critical temperature we expect the Heisenberg fixed point to dominate the dynamics, but the other two can be relevant if the initial values of the running parameters are sufficiently close to them. In the parameter regions $x>2$, $x<-1$ we expect first-order phase transitions. In the following sections we shall verify the above conclusions with improved quantitative accuracy.

IV. TRUNCATIONS OF THE EVOLUTION EQUATION

We proceed now to a more detailed study of the evolution equation and its truncations. As we have discussed at the end of Sec. II, we parametrize the effective average potential by its minimum and its derivatives at the minimum. For this work we shall use a truncation that preserves up to second derivatives of the potential.

In the *symmetric regime* (which we denote by S) the minimum of the potential is at $\rho_{10}(k)=\rho_{20}(k)=0$ and we use the definitions of Eq. (3.1). The evolution equations in arbitrary dimension d automatically preserve the symmetry. They read

$$\frac{d\bar{m}^2}{dt}=v_d k^{d-2}(4+x)\bar{\lambda}L_1^d(\bar{m}^2), \tag{4.1}$$

$$\frac{d\bar{\lambda}}{dt}=-v_d k^{d-4}(10+2x+x^2)\bar{\lambda}^2 L_2^d(\bar{m}^2), \tag{4.2}$$

$$\frac{dx}{dt}=v_d k^{d-4}(x+1)x(x-2)\bar{\lambda}L_2^d(\bar{m}^2), \tag{4.3}$$

with the dimensionless integrals $L_n^d(w)$ given by

$$L_n^d(w)=-nk^{2n-d}\pi^{-d/2}\Gamma\left(\frac{d}{2}\right)\int d^dq\frac{\partial P}{\partial t}(P+w)^{-(n+1)}$$

$$=-nk^{2n-d}\int_0^\infty dx\; x^{d/2-1}\frac{\partial P}{\partial t}(P+w)^{-(n+1)}. \tag{4.4}$$

Here P is given by Eq. (2.11), and

$$v_d^{-1}=2^{d+1}\pi^{d/2}\Gamma\left(\frac{d}{2}\right). \tag{4.5}$$

In the *spontaneously broken regime* there are two possibilities consistent with the symmetry:

(I) In the M regime the minimum of the potential is located symmetrically between the ρ axes at $\rho_{10}(k)=\rho_{20}(k)=\frac{1}{2}\rho_0(k)$. We define the couplings

$$\bar{\lambda}(k)=U_{11}(\rho_0)=U_{22}(\rho_0)>0,$$

$$\bar{g}(k)=U_{12}(\rho_0),\quad x(k)=\frac{\bar{g}(k)}{\bar{\lambda}(k)}-1. \tag{4.6}$$

The requirement that the point $(\frac{1}{2}\rho_0,\frac{1}{2}\rho_0)$ is the minimum of the potential imposes $x<0$, while the potential is bounded at infinity for $x>-2$. For $x=0$ the symmetry of the theory is increased to O(2) and the potential develops a series of degenerate minima along the circle $\rho_{10}+\rho_{20}=\rho_0$. For $x=-1$ the theory decomposes into two disconnected $Z_2(\phi_{1,2}\leftrightarrow-\phi_{1,2})$-symmetric models. The mass eigenvalues are given by $M_1^2=(2+x)\bar{\lambda}\rho_0$, $M_2^2=-x\bar{\lambda}\rho_0$. The evolution equation for the minimum $\rho_0(k)$ is obtained by considering the total t derivative of the conditions $\partial U_k/(\partial\rho_1)\rho_0=\partial U_k/(\partial\rho_2)\rho_0=0$ [6,8]. Again, the truncated evolution equations automatically preserve the symmetry and read

$$\frac{d\rho_0}{dt}=-v_d k^{d-2}\left(3L_1^d[(2+x)\bar{\lambda}\rho_0]+\frac{2-x}{2+x}L_1^d(-x\bar{\lambda}\rho_0)\right), \tag{4.7}$$

$$\frac{d\bar{\lambda}}{dt}=-v_d k^{d-4}\frac{3x\bar{\lambda}}{\rho_0}\frac{1+\frac{x}{4}}{1+x}\{L_1^d[(2+x)\bar{\lambda}\rho_0]-L_1^d(-x\bar{\lambda}\rho_0)\}$$
$$-v_d k^{d-4}\bar{\lambda}^2\left[9\left(1+\frac{x}{2}\right)^2 L_2^d[(2+x)\bar{\lambda}\rho_0]\right.$$
$$\left.+\left(1-\frac{x}{2}\right)^2 L_2^d(-x\bar{\lambda}\rho_0)\right], \tag{4.8}$$

$$\frac{dx}{dt}=v_d k^{d-2}\frac{3}{\rho_0}\frac{2+x}{1+x}\left(x+\frac{x^2}{4}\right)\{L_1^d[(2+x)\bar{\lambda}\rho_0]$$
$$-L_1^d(-x\bar{\lambda}\rho_0)\}+v_d k^{d-4}x\bar{\lambda}\left[9\left(1+\frac{x}{2}\right)^2 L_d[(2+x)\bar{\lambda}\rho_0]\right.$$
$$\left.+\left(1-\frac{x}{2}\right)^2 L_2^d(-x\bar{\lambda}\rho_0)\right]. \tag{4.9}$$

For $x=0$ the above evolution equations reproduce the equations of the O(2)-symmetric theory, while for $x=-1$ they reproduce those of the Z_2-symmetric one (compare with Refs. [6,10]).

(II) In the regime which we denote by AX, two degenerate minima of the potential exist on each one of the ρ axes. Without loss of generality we concentrate on the minimum at $\rho_{10}(k)=\rho_0(k), \rho_{20}(k)=0$. At the level of truncations that we are considering, the remaining parameters of the theory are conveniently defined according to Eq. (4.6) and

$$\bar{m}_2^2(k)=U_2(\rho_0). \tag{4.10}$$

The symmetry demands that for the truncated potential

$$\bar{m}_2^2(k)=x(k)\bar{\lambda}(k)\rho_0(k). \tag{4.11}$$

The requirement that the point $(\rho_0,0)$ is the minimum of the potential imposes $x>0$. As before, for $x=0$ the symmetry of the theory is increased to O(2). The mass eigenvalues are given by $M_1^2=2\bar{\lambda}\rho_0, M_2^2=x\bar{\lambda}\rho_0$. At this point we encounter a difficulty. The derivation of truncated evolution equations is hindered by the fact that the parametrization around a minimum located on one of the axes is asymmetric between the two fields. As a result the symmetry $(\phi_1\leftrightarrow\phi_2)$, is not maintained by the evolution equations at each level of the truncations. More specifically, the flow equations for the couplings $U_{11}(\rho_0)$, $U_{22}(\rho_0)$ are different. Also, Eq. (4.11) is not preserved by the evolution equation. This is not surprising, since these relations are not expected to hold for the exact potential without truncation. It is easy to see that they are altered as soon as third derivatives of the potential are included. This is in contrast with what happens in the M regime, where the formulation is symmetric between the two fields. For example, in the M regime the couplings U_{11}, U_{22} are expected to remain equal at every level of truncations, and indeed this is guaranteed by the evolution equations. The above remarks indicate a natural method of preserving the $(1\leftrightarrow-1,\ 2\leftrightarrow-2,\ 1\leftrightarrow2)$ symmetry in the AX regime. A redefinition of fields and couplings in analogy to Eqs. (1.5), (1.6) results in a rotation of the axes by 45°, thus transforming the AX into the M regime. The evolution equations for the redefined quantities have already been worked out and are given by Eqs. (4.7)–(4.9). By simply rewriting them in terms of the old quantities we obtain

$$\frac{d\rho_0}{dt}=-v_d k^{d-2}[3L_1^d(2\bar{\lambda}\rho_0)+(1+x)L_1^d(x\bar{\lambda}\rho_0)], \tag{4.12}$$

$$\frac{d\bar{\lambda}}{dt}=-v_d k^{d-4}\bar{\lambda}^2[9L_2^d(2\bar{\lambda}\rho_0)+(1+x)^2L_2^d(x\bar{\lambda}\rho_0)], \tag{4.13}$$

$$\frac{dx}{dt}=v_d k^{d-2}\frac{6}{\rho_0}\frac{x+\frac{x^2}{4}}{1-\frac{x}{2}}[L_1^d(2\bar{\lambda}\rho_0)-L_1^d(x\bar{\lambda}\rho_0)]$$
$$+v_a k^{d-4}x\bar{\lambda}[9L_2^d(2\bar{\lambda}\rho_0)+(1+x)^2L_2^d(x\bar{\lambda}\rho_0)]. \tag{4.14}$$

For $x=0$ the above evolution equations reproduce the ones of the O(2)-symmetric theory. Another special point is $x=2$ for which the theory, when expressed in terms of the redefined fields $\tilde{\phi}_1,\tilde{\phi}_2$, decomposes into two disconnected $Z_2(\tilde{\phi}_{1,2}\leftrightarrow-\tilde{\phi}_{1,2})$-symmetric models. We should point out that Eqs. (4.12)–(4.14) could have been obtained by defining $\bar{\lambda}=U_{11}(\rho_0)$ and $x=U_2(\rho_0)/U_{11}(\rho_0)\rho_0$ [in agreement with Eq. (4.11)] and inserting Eqs. (4.6), (4.10) in the RHS of the flow equations. The advantage of the redefinition is that it makes transparent how this apparently arbitrary choice of parameters preserves the original symmetry at this truncation level.

In the following sections we shall use the evolution equations (4.1)–(4.3), (4.7)–(4.9), and (4.12)–(4.14), for the S, M, and AX regimes respectively, in order to obtain the renormalized theory in its various phases.

V. THE INTEGRALS L_n^d FOR ZERO AND NONZERO TEMPERATURE

The integrals $L_n^d(w)$, defined in Eq. (4.4), have been discussed extensively in Refs. [8,10,33] [for various shapes of the infrared regulating function $R_k(q)$, for which Eqs. (2.2), (2.3) are the most natural choice [9]]. We refer the reader to Appendix A of Ref. [10] for a summary of their properties. The most interesting property of $L_n^d(w)$, for our discussion, is that they fall off for large values of w/k^2, following a power law. As a result they introduce threshold behavior for the contributions of massive modes to the evolution equations. It is obvious from Eqs. (4.1)–(4.3), (4.7)–(4.9), and (4.12)–(4.14), for the S, M, and AX regimes, respectively, that the various contributions to the evolution equations involve L_n^d integrals with the mass eigenvalues as their arguments. When the running squared mass of a massive mode

becomes much larger than the scale k^2 (at which the system is probed), these contributions vanish and the massive modes decouple. We evaluate the integrals $L_n^d(w)$ numerically and use numerical fits for the solution of the evolution equations.

In order to extend the formalism of the previous section to nonzero temperature we only need to recall that, in Euclidean formalism, nonzero temperature T results in periodic boundary conditions in the time direction (for bosonic fields), with periodicity $1/T$ [34]. This leads to a discrete spectrum for the zero component of the momentum q_0:

$$q_0 \to 2\pi m T, \quad m = 0, \pm 1, \pm 2, \ldots \ . \tag{5.1}$$

As a consequence the integration over q_0 is replaced by a summation over the discrete spectrum

$$\int \frac{d^d q}{(2\pi)^d} \to T \sum_m \int \frac{d^{d-1}\vec{q}}{(2\pi)^{d-1}}. \tag{5.2}$$

With the above remarks in mind we can easily generalize our master equation (2.10) in order to take into account the temperature effects. For the temperature-dependent effective average potential $U_k(\rho_1, \rho_2, T)$ we obtain

$$\frac{\partial}{\partial t} U_k(\rho_1, \rho_2, T) = \frac{1}{2}(2\pi)^{-(d-1)} T \sum_m \int d^{d-1}\vec{q} \left(\frac{1}{P + M_1^2} + \frac{1}{P + M_2^2} \right) \frac{\partial}{\partial t} R_k, \tag{5.3}$$

with the implicit replacement

$$q^2 \to \vec{q}^2 + 4\pi^2 m^2 T^2 \tag{5.4}$$

in Eqs. (2.2), (2.3), and (2.11) for R_k and P. Again, the usual temperature-dependent effective potential [2–4] is obtained from $U_k(\rho_1, \rho_2, T)$ in the limit $k \to 0$. As before, we can parametrize $U_k(\rho_1, \rho_2, T)$ in terms of its minimum and its derivatives at the minimum. The evolution equations are given by (4.1)–(4.3), (4.7)–(4.9), and (4.12)–(4.14), with the obvious generalizations

$$\rho_0(k) \to \rho_0(k,T), \quad \bar{m}^2(k) \to \bar{m}^2(k,T), \quad \bar{\lambda}(k) \to \bar{\lambda}(k,T), \quad x(k) \to x(k,T). \tag{5.5}$$

The L_n^d integrals for nonvanishing temperature read

$$L_n^d(w,T) = -2nk^{2n-d}\pi^{-d/2+1}\Gamma\left(\frac{d}{2}\right) T \sum_m \int d^{d-1}\vec{q} \frac{\partial P}{\partial T} \times (P + w)^{-(n+1)}, \tag{5.6}$$

where the implicit replacement (5.4) is assumed in P. Their basic properties can be established analytically. For $T \ll k$ the summation over discrete values of m in the expression (5.6) is equal to the integration over a continuous range of q_0 up to exponentially small corrections. Therefore

$$L_n^d(w,T) = L_n^d(w) \quad \text{for} \quad T \ll k. \tag{5.7}$$

In the opposite limit $T \gg k$ the summation over m is dominated by the $m = 0$ contribution. Terms with nonzero values of m are suppressed by $\sim \exp[-(mT/k)^2]$. The leading contribution gives the simple expression

$$L_n^d(w,T) = \frac{v_{d-1}}{v_d} \frac{T}{k} L_n^{d-1}(w) \quad \text{for} \quad T \gg k, \tag{5.8}$$

with v_d defined in (4.5). The two regions of T/k in which $L_n^d(w,T)$ is given by the equations (5.7), (5.8) are connected by a small interval, in which the exponential corrections result in a more complicated dependence on w and T. The above conclusions are verified by a numerical calculation of $L_1^4(w,L)$. In Fig. 2 we plot[5] $L_1^4(w,T)/L_1^4(w)$ as a function of T/k, for various values of w/k^2. We distinguish three regions.

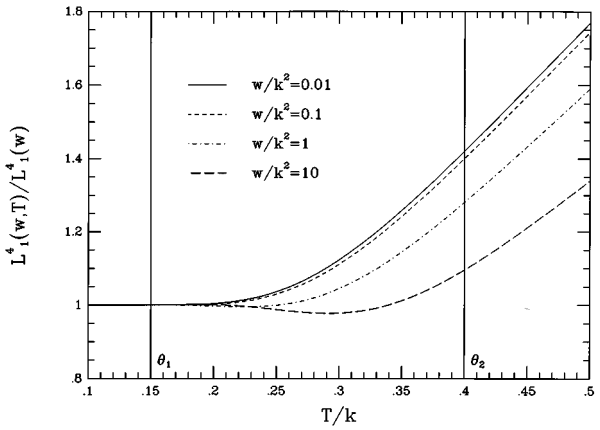

FIG. 2. $L_1^4(w,T)/L_1^4(w)$ as a function of T/k, for various values of w/k^2.

(a) $T/k \leqslant \theta_1$. This is the *low temperature region* where $L_{1,2}^4(w,T)$ are very well approximated by their zero temperature value. We take $\theta_1 = 0.15$ and use $L_{1,2}^4(w,0)$ in the evolution equations for $k \geqslant T/\theta_1$.

(b) $\theta_1 < T/K < \theta_2$. In the *threshold region* we perform a numerical fit of the curve corresponding to $w = 0$ which we use for all values of w. This is a good approximation since the relevant w/k^2 turns out to be small in this region (see next sections).

(c) $T/k \geqslant \theta_2$. We take $\theta_2 = 0.4$. For the *high temperature regions* we use, for the numerical solution of the evolution equations,

$$L_{1,2}^4(w,T) = 4\frac{T}{k} L_{1,2}^3(w). \tag{5.9}$$

The three-dimensional character of the effective theory for modes with $q^2 \ll T^2$ manifests itself in the appearance of the three-dimensional momentum integrals. It acquires here a precise quantitative meaning.

[5]Comparison with results presented in Ref. [6] shows that the form of these functions depends on the details of the infrared regulating function $R_k(q)$. However, the physical results, which are obtained when the cutoff is removed, are independent of the shape of the cutoff. This will be apparent in the next sections and is a verification of the scheme independence of our conclusions.

We have now developed the necessary formalism for the study of the four-dimensional zero and nonzero temperature theory. In the following two sections we study the evolution of the running parameters of the theory, which leads to the determination of the renormalized theory at zero and nonzero temperature.

VI. THE RUNNING IN THE LOW-TEMPERATURE AND THRESHOLD REGIONS

In Sec. IV we derived the zero temperature evolution equations for the parameters (masses, vacuum expectation values, and couplings) of the truncated theory as a function of the scale k in the various regimes (S,M,AX). In Sec. V we generalized the formalism in order to take into account nonzero temperature effects. The evolution equations can be solved for a given set of initial conditions, specified as the values of the running parameters at a scale equal to the ultraviolet cutoff of the theory $(k=\Lambda)$. As we pointed out in Sec. II, at this scale the effective average action is equal to the classical action. Therefore, the initial values for the parameters correspond to their classical (or bare) values. Also, the discussion in Sec. V has shown that in the low-temperature region $(k \geqslant T/\theta_1)$ there is no difference between the zero and nonzero temperature theory. As a result, we can define the theory in terms of the classical values of its parameters at $k=\Lambda \gg T$, independently of the temperature. The integration of the evolution equations gives the running couplings at lower scales. No temperature effects are observed in the evolution inside the low-temperature region $(k \geqslant T/\theta_1)$. We can, therefore, use the values of the running couplings at $k=T/\theta_1$ for the definition of the theory, since they are in one-to-one correspondence with the classical couplings, independently of the temperature. This turns out to be the most convenient choice and we shall use it for the rest of the paper. The temperature starts to become important when the evolution enters the threshold region $(T/\theta_1 > k > T\theta_2)$. In the high-temperature region $(k \leqslant T/\theta_2)$ the evolution is effectively three-dimensional, as we discussed in Sec. V. Finally, in the limit $k \to 0$ the effective average action becomes the effective action, and the integration of the evolution equations gives the renormalized values for the couplings at various temperatures. All the information on the various phases of the theory is contained in these renormalized couplings and their temperature dependence.

We have seen in the introduction and in Sec. IV that the AX regime $(x>0)$ and the M regime $(x<0)$ can be mapped onto each other through a simple redefinition of the fields [in analogy to Eqs. (1.5), (1.6)]. For this reason, the physical behavior in the two regimes is the same. For example, the cubic and Ising fixed points generate the same universal behavior (characteristic of a Z_2-symmetry scalar theory). For this reason, we shall concentrate on the region $x>0$ only. All the results can be easily extended to the region $x<0$, through transformations analogous to Eqs. (1.5), (1.6).

Since we are interested in symmetry restoration at nonzero temperature, we first consider the theory in the spontaneously broken regime. The evolution equations in the AX regime (which is the relevant one for $x>0$) in four dimensions and nonzero temperature can be easily derived from Eqs. (4.12)–(4.14) and read

$$\frac{d\rho_0}{dt} = -v_4 k^2 [3L_1^4(2\bar{\lambda}\rho_0) t_1(2\bar{\lambda}\rho_0, T) + (1+x) L_1^4(x\bar{\lambda}\rho_0) t_1(x\bar{\lambda}\rho_0, T)], \tag{6.1}$$

$$\frac{d\bar{\lambda}}{dt} = -v_4 \bar{\lambda}^2 [9L_2^4(2\bar{\lambda}\rho_0) t_2(2\bar{\lambda}\rho_0, T) + (1+x)^2 L_2^4(x\bar{\lambda}\rho_0) t_2(x\bar{\lambda}\rho_0, T)], \tag{6.2}$$

$$\frac{dx}{dt} = v_4 \frac{6}{\rho_0} \frac{x+\frac{x^2}{4}}{1-\frac{x}{2}} [L_1^4(2\bar{\lambda}\rho_0) t_1(2\bar{\lambda}\rho_0, T) - L_1^4(x\bar{\lambda}\rho_0) t_1(x\bar{\lambda}\rho_0, T)] + v_4 x \bar{\lambda} [9L_2^4(2\bar{\lambda}\rho_0) t_2(2\bar{\lambda}\rho_0, T) + (1+x)^2 L_2^4(x\bar{\lambda}\rho_0) t_2(x\bar{\lambda}\rho_0, T)], \tag{6.3}$$

where $v_4 = 1/32\pi^2$. We have not indicated explicitly the k and T dependence of the running parameters $\rho_0(k,T)$, $\bar{\lambda}(k,T)$, $x(k,T)$. They are defined at zero temperature according to Eqs. (4.6), (4.10), and generalized for nonzero temperature according to Eq. (5.5). The functions $t_{1,2}$ are defined as

$$t_n(w,T) = \frac{L_n^4(w,T)}{L_n^4(w)}, \tag{6.4}$$

with $t_1(w,T)$ plotted in Fig. 2.

At zero temperature one has $t_n(w,0)=1$ and the evolution equations have only one infrared attractive fixed point, the Gaussian one. In the limit of small $\bar{\lambda}$ we shall neglect the slow logarithmic running of $\bar{\lambda}$, which is eventually stopped by the mass terms in the threshold functions $L_{1,2}^4$. Similarly the running of x can also be neglected since it is suppressed by $\bar{\lambda}/32\pi^2$. [For small $\bar{\lambda}$ the difference of the two L_1^4 functions in the first line of Eq. (6.3) gives a contribution $\propto \bar{\lambda} L_2^4(0)$.] For large $\bar{\lambda}$ the evolution equations can be integrated numerically and the small resulting corrections can be reliably computed. This has been done in Ref. [6] for the O(N)-symmetric scalar theory. In this paper we concentrate on small couplings for which analytical expressions can be obtained. Equation (6.1) can be integrated easily for small $\bar{\lambda}$ and we obtain $[L_1^4(0) = -2]$

$$\rho_0(k,0) = \rho_0\left(\frac{T}{\theta_1}\right) + \frac{1}{32\pi^2}(x+4)\left[k^2 - \left(\frac{T}{\theta_1}\right)^2\right], \tag{6.5}$$

where we used the point $k=T/\theta_1$ instead of $k=\Lambda$ to start the evolution, as we have explained in the first paragraph of this section. We define the renormalized couplings of the theory in the limit $k \to 0$ as[6]

[6] In the case that Goldstone modes are present (as for $x=0$) the couplings are defined at some appropriate nonzero k. The same applies for nonzero temperature. This does not affect our results for small $\bar{\lambda}$. For a detailed discussion see Ref. [6].

$$\rho_0=\rho_0(0,0),\quad \lambda_R=\bar{\lambda}(0,0),\quad x_R=x(0,0), \tag{6.6}$$

and conclude that

$$\rho_0\left(\frac{T}{\theta_1}\right)=\rho_0+\frac{1}{32\pi^2}(x_R+4)\left(\frac{T}{\theta_1}\right)^2. \tag{6.7}$$

At nonzero temperature, the evolution in the low-temperature region ($k\geqslant T/\theta_1$) is identical to the zero-temperature case. In the threshold region ($T/\theta_1>k>T/\theta_2$), the form of $t_{1,2}(w,T)$ is not given by a simple analytical expression. For small λ we neglect the running of λ,x in this region and find

$$\begin{aligned}\rho_0\left(\frac{T}{\theta_2},T\right)&=\rho_0\left(\frac{T}{\theta_1}\right)-\frac{1}{16\pi^2}(x+4)T^2I\\&=\rho_0+\frac{1}{16\pi^2}(x_R+4)T^2\left(\frac{1}{2\theta_1^2}-I\right),\\ \bar{\lambda}\left(\frac{T}{\theta_2},T\right)&=\bar{\lambda}\left(\frac{T}{\theta_1}\right)=\lambda_R,\quad x\left(\frac{T}{\theta_2},T\right)=x\left(\frac{T}{\theta_1}\right)=x_R,\end{aligned} \tag{6.8}$$

where

$$I=\int_{1/\theta_2}^{1/\theta_1}dy\ y t_1\left(0,\frac{1}{y}\right), \tag{6.9}$$

and we have made use of the fact that $t_1^4(w,T)$ depends on T only through the combination T/k. The integral I can be evaluated numerically. For $\theta_1=0.15$, $\theta_2=0.4$ we find $I=19.97$. Equation (6.8) set the initial values for the evolution in the high-temperature region.

VII. THE RUNNING IN THE HIGH-TEMPERATURE REGION

In the high-temperature region ($k\leqslant T/\theta_2$) the functions $L_{1,2}^4(w,T)$ are given by the simplified expression (5.9). We can rewrite Eqs. (6.1)–(6.3) in terms of effective three-dimensional couplings

$$\rho_0'(k,T)=\frac{\rho_0(k,T)}{T},\quad \bar{\lambda}'(k,T)=\bar{\lambda}(k,T)T,$$

$$\bar{g}'(k,T)=\bar{g}(k,T)T,\quad x(k,T)=\frac{\bar{g}'(k,T)}{\bar{\lambda}'(k,T)}-1. \tag{7.1}$$

The resulting flow equations are exactly the ones of the three-dimensional theory at zero temperature, as given by Eqs. (4.12)–(4.14) with $d=3$. In order to make their fixed-point structure more transparent we define the dimensionless parameters

$$\begin{aligned}\kappa(k,T)&=\frac{\rho_0'(k,T)}{k}=\frac{\rho_0(k,T)}{kT},\\ \lambda(k,T)&=\frac{\bar{\lambda}'(k,T)}{k}=\frac{\bar{\lambda}(k,T)T}{k},\\ g(k,T)&=\frac{\bar{g}'(k,T)}{k}=\frac{\bar{g}(k,T)T}{k}.\end{aligned} \tag{7.2}$$

In terms of these we obtain the scale-invariant form of the evolution equations

$$\frac{d\kappa}{dt}=-\kappa-v_3[3L_1^3(2\lambda\kappa)+(1+x)L_1^3(x\lambda\kappa)], \tag{7.3}$$

$$\frac{d\lambda}{dt}=-\lambda-v_3\lambda^2[9L_2^3(2\lambda\kappa)+(1+x)^2L_2^3(x\lambda\kappa)], \tag{7.4}$$

$$\begin{aligned}\frac{dx}{dt}=v_3\frac{6}{\kappa}\frac{x+\frac{x^2}{4}}{1-\frac{x}{2}}[L_1^3(2\lambda\kappa)-L_1^3(x\lambda\kappa)]+v_3x\lambda[9L_2^3(2\lambda\kappa)\\+(1+x)^2L_2^3(x\lambda\kappa)].\end{aligned} \tag{7.5}$$

No explicit dependence on the scale k appears on the r.h.s.

The first of the above equations defines a critical surface $\kappa_{\rm cr}=\kappa_{\rm cr}(\lambda,x)$. It consists of the points $\kappa_{\rm cr}$ for which the solution of Eqs. (7.3)–(7.5) approaches, for large negative t, a scaling solution with κ, λ, and x independent of t. (For a weakly first-order transition the scaling holds only approximately.) Every point on the critical surface is unstable in the κ direction. Trajectories which start at $\kappa>\kappa_{\rm cr}$ continue towards the region of large κ, in such a way that $\rho_0(k,T)=\kappa(k,T)Tk$ reaches asymptotically a constant value for $k\to0$. As a result the renormalized theory settles down in the phase with spontaneous symmetry breaking. If the evolution starts at $\kappa<\kappa_{\rm cr}$, the flows cross the surface $\kappa=0$ at some finite k_s. From this point on the system is in the symmetric regime. In order to continue the evolution, we define appropriate parameters according to Eq. (3.1) and effective three-dimensional couplings according to Eq. (7.1). The resulting evolution equations are the ones for the three-dimensional theory in the symmetric regime, as given by Eqs. (4.1)–(4.3) with $d=3$. We define the dimensionless parameter

$$m^2(k,T)=\frac{\bar{m}^2(k,T)}{k^2}, \tag{7.6}$$

and $\lambda(k,T)$, $g(k,T)$ according to Eq. (7.2). In terms of these quantities the evolution equations in the symmetric regime are given by Eqs. (3.3)–(3.5). We start the evolution in this regime at $k=k_s$ with $m^2(k_s,T)=0$ and $\lambda(k_s,T)$, $x(k_s,T)$ taking their values at the end of the running in the spontaneously broken regime. For $k\to0$ the evolution is stopped by the mass terms in the threshold functions $L_{1,2}^3$ and the theory settles down in the symmetric phase. Obviously the critical temperature $T_{\rm cr}$ is related to $\kappa_{\rm cr}$ [for given $\lambda(T_{\rm cr}/\theta_2)$, $x(T_{\rm cr}/\theta_2)$] by

$$\kappa\left(\frac{T_{\rm cr}}{\theta_2}\right)=\kappa_{\rm cr}. \tag{7.7}$$

On the critical surface there are two fixed points with at least one attractive direction for the flow towards the infrared ($k\to0$): (a) the cubic fixed point located at

$$\kappa_c=5.674\times10^{-2},\quad \lambda_c=8.747,\quad x_c=2, \tag{7.8}$$

and (b) the Heisenberg fixed point located at

$$\kappa_H = 4.486 \times 10^{-2}, \quad \lambda_H = 15.265, \quad x_H = 0. \quad (7.9)$$

Both fixed points are attractive in the λ direction, but the cubic fixed point is unstable in the x direction while the Heisenberg one is stable. For fixed x there is also the infrared unstable Gaussian fixed point. It is located at

$$\kappa_G = -v_3(x+4)L_1^3(0) = \frac{1}{8\pi^{3/2}}(x+4)\lambda_G = 0. \quad (7.10)$$

These fixed points are the same as the ones observed in Sec. III. The only difference lies in the parametrization. In Sec. III we used an expansion around the origin of the potential and the evolution equations in the symmetric regime. For this reason the fixed points appeared for negative values of the mass parameter (the curvature at the origin), indicating a minimum away from the origin. In this section we rely on a parametrization around the minimum of the potential, which results in increased quantitative accuracy for the truncation.

The flows on the critical surface are qualitatively similar to those in Fig. 1 for $x>0$. There are two disconnected regions:

(a) $2>x>0$. The trajectories flow away from the cubic fixed point and towards the Heisenberg fixed point. This region corresponds to a second order phase transition.

(b) $x>2$. The trajectories flow away from the cubic fixed point and into a region of small λ and large x. Similarly to our discussion in Sec. III, we expect $\lambda(k,T)$ to become negative at some finite k. This indicates that the minimum of the potential becomes unstable (it turns into a maximum). Our crude truncation is not sufficient for the investigation of this situation, since the higher derivatives of the potential are important. A detailed study is presented in Ref. [35] for the four-dimensional theory at zero temperature. The dimensionality of the theory is not crucial for the qualitative behavior in this region of parameter space. The first term in the RHS of Eq. (7.4) (which is present only for the effectively three-dimensional theory) is not important for large x. The second term, which drives the dynamics, is the same as for the four-dimensional theory (with the replacement of $v_3 L_1^3$ by $v_4 L_1^4$ generating only quantitative corrections). In Ref. [35] higher derivatives of the potential are taken into account. Also, a parametrization is used which simultaneously follows the evolution of the potential at its minimum at nonzero $\rho_0(k,T)$ and at the origin. This permits the study of the global properties of the potential. It is found that during the evolution in the region $x>2$ a second minimum appears at the origin which subsequently becomes the absolute minimum of the potential. This results in a discontinuity in the order parameter and a first-order phase transition. At some point in the evolution, λ turns negative and the minimum at nonzero ρ_0 disappears. From this point on the deeper minimum at zero is the only minimum. During the whole evolution the higher derivatives stay positive guaranteeing that the potential remains bounded. We cannot reproduce the above picture within the crude truncation of a quartic polynomial for the potential. Instead we shall give in Sec. XI an approximate solution of the evolution equation for the potential in this region, which will demonstrate the existence of the first-order transition.

VIII. THE CRITICAL TEMPERATURE

A quantity which can be easily calculated from the discussion in the last two sections is the critical temperature for the phase transitions. From Eqs. (6.8) and (7.2) we obtain

$$\kappa\left(\frac{T}{\theta_2},T\right) = \theta_2\frac{\rho_0}{T^2} + \frac{\theta_2}{16\pi^2}\left(\frac{1}{2\theta_1^2} - I\right)(x_R+4),$$

$$\lambda\left(\frac{T}{\theta_2},T\right) = \theta_2\lambda_R, \quad x\left(\frac{T}{\theta_2},T\right) = x_R. \quad (8.1)$$

For small λ the critical surface, which separates the symmetric phase from the phase with spontaneous symmetry breaking, goes through the Gaussian fixed point given by Eq. (7.10). The critical temperature can be computed as the temperature for which $\kappa(T/\theta_2,T)$ coincides with the Gaussian fixed point κ_G. This gives

$$\frac{T_{\rm cr}^2}{\rho_0} = \frac{C}{x_R+4}, \quad C^{-1} = \frac{1}{8\pi^2}\left[\frac{\sqrt{\pi}}{\theta_2} - \frac{1}{2}\left(\frac{1}{2\theta_1^2} - I\right)\right], \quad (8.2)$$

independently of λ_R. Substitution of the values $\theta_1 = 0.15$, $\theta_2 = 0.4$, $I = 19.97$, which we computed in the first part of this section, gives

$$C = 23.89. \quad (8.3)$$

We should point out that the above value for the critical temperature is not strictly valid for $x_R>2$. In this region the first-order phase transition occurs for $\kappa(T/\theta_2,T)$ slightly above the critical surface. As a result the transition takes place at a temperature slightly lower than the one given by Eq. (8.2). In the language of the effective three-dimensional theory, the distance from the phase transition can be parametrized, for small λ_R, in terms of $\delta\kappa_{\rm cr} = \kappa(T/\theta_2,T) - \kappa_G$. We establish the connection between this quantity and the temperature as

$$\delta\kappa_{\rm cr} = \kappa\left(\frac{T}{\theta_2},T\right) - \kappa_G = \theta_2\rho_2\left(\frac{1}{T^2} - \frac{1}{T_{\rm cr}^2}\right). \quad (8.4)$$

The critical temperature can be calculated in high-temperature perturbation theory through the perturbative expansion of the effective potential [5] and its generalization to nonzero temperature [2–4]. The calculation is straightforward and we do not present the details here. When the leading term in the high-temperature expansion of the one-loop contribution to the effective potential is retained, the critical temperature is found to be

$$\frac{T_{\rm cr}^2}{\rho_0} = \frac{24}{x_R+4}. \quad (8.5)$$

This value is in excellent agreement with our result. The slight discrepancy is due to small deviations of the form of $L_1^4(w,T)$ that we have used from the exact expression, and

could probably be removed by using lower θ_1 and larger θ_2. It is well known that the perturbative expansion of the effective potential breaks down near the critical temperature for a second or weakly first-order phase transition, due to infrared divergences [6]. The surprising accuracy of the perturbative estimate for the critical temperature is due to the fact that the infrared divergences appear at temperatures $|T-T_{\rm cr}|/T_{\rm cr}=\mathcal{O}(\lambda_R)$. For sufficiently small λ_R the location of the transition can be accurately computed. However, naive perturbative predictions for the details of the transition (even its order) can be misleading. This is the case for our model, for which the next terms in the naive high-temperature expansion of the perturbative result fail to reproduce even the correct qualitative picture[7] (apart from a small region in parameter space which will be discussed at the end of the next section). We emphasize that our approach may also be used for large values of λ_R not so easily accessible to perturbation theory. In this case κ_G should be replaced by the relevant exact point on the critical surface $\kappa_{\rm cr}$.

IX. SECOND-ORDER PHASE TRANSITION AND THE CRITICAL BEHAVIOR

Let us briefly summarize the main results of the previous sections. We have considered theories which at zero temperature are in the phase with spontaneous symmetry breaking corresponding to the *AX* regime. They are defined in terms of the classical (bare) parameters at the ultraviolet cutoff $\Lambda \gg T$. The renormalized parameters are obtained by solving the evolution equations from $k=\Lambda$ to $k=0$. In the low-temperature region ($\Lambda \gtrsim k \gtrsim T/\theta_1$) there is no difference between the zero and nonzero temperature case for the evolution of the parameters of the theory. The first temperature effects are observed in the threshold region ($T\theta_1 > k > T/\theta_2$). For small λ_R the values of the running parameters at the beginning of the evolution in the high-temperature region ($k=T/\theta_2$) can be expressed in terms of the renormalized parameters of the zero-temperature theory. The relation is given by Eq. (6.8). In the high-temperature region ($k \lesssim T/\theta_2$) the character of the evolution is effectively three-dimensional and is governed by the fixed points of the three-dimensional theory. These are most transparent in terms of the dimensionless parameters defined in Eq. (7.2). The evolution equations are given by Eqs. (7.3)–(7.5). These equations define a critical surface $\kappa_{\rm cr}=\kappa_{\rm cr}(\lambda,x)$, which is unstable in the κ direction and separates the phase with spontaneous symmetry breaking from the symmetric one. The system ends up in either phase depending on the values of the running parameters at $k=T/\theta_2$. For small λ the critical surface goes through the Gaussian fixed point given by Eq. (7.10). As a result, for small λ_R the crucial quantity is the distance from the critical surface $\delta\kappa_{\rm cr}=\kappa(T/\theta_2,T)-\kappa_G$. For $\delta\kappa_{\rm cr}>0$ the theory ends up in the phase with spontaneous symmetry breaking. For $\delta\kappa_{\rm cr}<0$ it ends up in the symmetric one. There is a direct connection between $\delta\kappa_{\rm cr}$ and the distance from the critical temperature, which is expressed in Eq. (8.4).

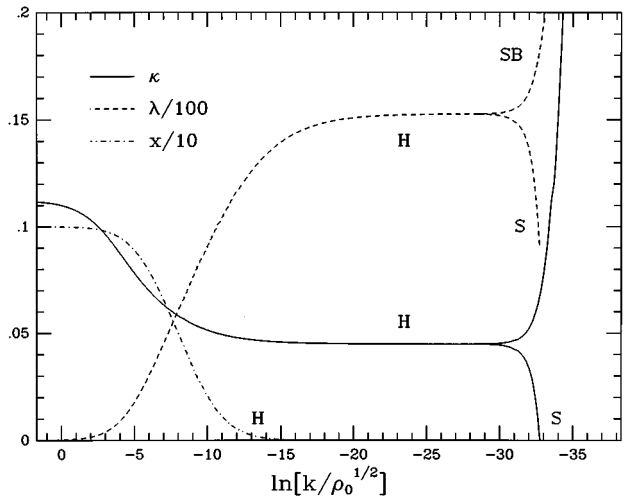

FIG. 3. The evolution of κ, λ, x in the high-temperature region, for temperatures slightly above and below the critical one, and $\lambda_R=0.01$, $x_R=1$, $T_{\rm cr}^2/\rho_0=4.78$. The system approaches the Heisenberg fixed point before deviating towards the symmetric phase or the phase with spontaneous symmetry breaking.

In this section we discuss the region in parameter space $0<x<2$ where the phase transition is second order. Sufficiently near to the critical temperature the evolution is governed by the Heisenberg fixed point. In Fig. 3 we plot the numerical solution of Eqs. (7.3)–(7.5) for the evolution in the high-temperature region, for a theory with zero temperature renormalized parameters $\lambda_R=0.01$, $x_R=1$ and critical temperature $T_{\rm cr}^2/\rho_0=4.78$. We display two trajectories, which start slightly above and below the critical surface (and therefore correspond to temperatures slightly below and above the critical one). We observe that the system flows towards the Heisenberg fixed point which is attractive in both the λ and x directions. It stays around this fixed point for several orders of magnitude in t and then deviates towards either the phase with spontaneous symmetry breaking or the symmetric one. During the "time" $t=\ln(k/\Lambda)$ that the system stays close the fixed point[8] it loses memory of the initial conditions of the evolution. Its dynamics is fixed solely by the fixed point, which has a purely three-dimensional character (as we demonstrated in Sec. VII). As a result we expect that the behavior of the theory near the critical temperature is independent of the details of the zero temperature theory. It must display universal critical behavior characteristic of systems with Heisenberg fixed point. As long as $\kappa(k,T)$ stays almost constant around its fixed point value κ_H and $k\to 0$ as $t\to-\infty$, the minimum of the effective average potential evolves towards zero according to

$$\rho_0(k,T)=\kappa_H k T. \tag{9.1}$$

[7]Perturbation theory for gap equations [37] may lead to more reliable results concerning the order of the transition but will fail for critical exponents unless the effectively three-dimensional running of the quaratic scalar coupling is properly included.

[8]We refer to $t=\ln(k/\Lambda)$ as "time" because it gives an intuitive picture of the evolution. It should not be confused with real time which plays no role in our study, as we are concerned with the static effective potential.

If the temperature is equal to the critical one, the system never leaves the fixed point and $\rho_0(0,T_{\rm cr})=0$. If the temperature is slightly below $T_{\rm cr}$, $\kappa(k,T)$ eventually runs away from the fixed point and diverges, so that $\rho_0(k,T)=\kappa(k,T)kT$ reaches a constant nonzero value as $k\to 0$. This value corresponds to the renormalized minimum of the effective potential at nonzero temperature and we denote it by

$$\rho_0(T)=\rho_0(0,T). \tag{9.2}$$

For a temperature slightly above $T_{\rm cr}$, $\kappa(k,T)$ [and therefore $\rho_0(k,T)$] runs to zero at a finite k_s. From this point on the system is in the symmetric regime and the appropriate evolution equations are given by Eqs. (3.3)–(3.5). We start the evolution in this regime at $k=k_s$ with $m^2(k_s,T)=0$ and $\lambda(k_s,T)$, $x(k_s,T)$ taking their values at the end of the running in the spontaneously broken regime. For $k\to 0$ the evolution is stopped by the mass terms in the threshold functions $L^3_{1,2}$ and the theory settles down in the symmetric phase. We define the renormalized mass in the symmetric phase as

$$m_R^2(T)=\bar{m}^2(0,T). \tag{9.3}$$

We also define the renormalized couplings in both phases as

$$\lambda_R(T)=\bar{\lambda}(0,T), \quad x_R(T)=x(0,T). \tag{9.4}$$

It is important to point out that, while the system is staying close to the fixed point, the coupling $\bar{\lambda}(k,T)$ evolves towards zero according to

$$\bar{\lambda}(k,T)=\lambda_H\frac{k}{T}. \tag{9.5}$$

As a result $\lambda_R(T)$ goes to zero as the critical temperature is approached. Its strong renormalization near $T_{\rm cr}$ provides the resolution of the problem of infrared divergences. The ratio $\lambda_R(T)T/m_R(T)$ does not diverge near the critical temperature, in contrast to $\lambda_R T/m_R(T)$. (Here λ_R is the renormalized coupling of the zero-temperature theory, which is approximately equal to the bare one for small couplings.) We shall not elaborate on this point, but we refer the reader to Ref. [6] for an extensive discussion. We also mention that as the temperature deviates from the critical one the system spends less "time" $t=\ln(k/\Lambda)$ near the critical point. Its flow deviates from those depicted in Fig. 3 at earlier stages. As a result the universal behavior ceases to dominate.

The behavior of the renormalized theory at various temperatures is shown in Fig. 4 for zero temperature parameters $\lambda_R=0.01$, $x_R=1$ and critical temperature $T_{\rm cr}^2/\rho_0=4.78$. We observe that $\rho_0(T)$ moves continuously to zero, indicating a second-order phase transition. The mass $m_R^2(T)$ is zero at $T_{\rm cr}$ and positive for larger temperatures. The quartic coupling $\lambda_R(T)$ stays close to its zero temperature value for most temperatures, but is strongly renormalized towards zero near $T_{\rm cr}$. The ratio of couplings $x_R(T)$ again takes its zero temperature value, unless the temperature is sufficiently close to $T_{\rm cr}$ for the flow to reach the Heisenberg fixed point. The universal behavior near $T_{\rm cr}$ can be parametrized by critical exponents, which we define similarly to Ref. [6] as

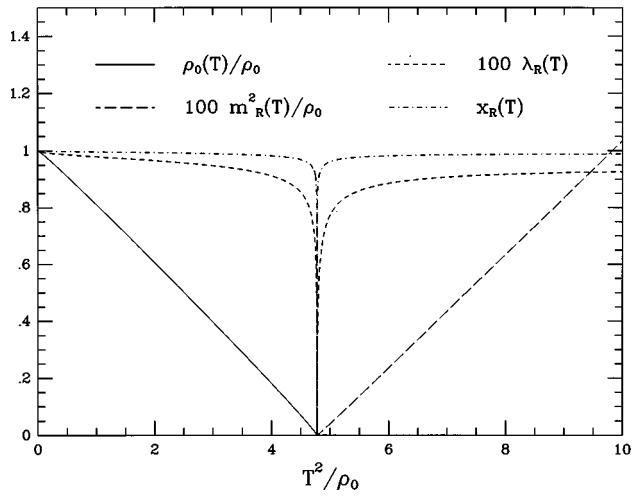

FIG. 4. The phase transition for a theory with $\lambda_R=0.01$, $x_R=1$, $T_{\rm cr}^2/\rho_0=4.78$.

$$\rho_0(T)\propto(T_{\rm cr}^2-T^2)^{2\beta}, \quad m_R^2(T)\propto(T^2-T_{\rm cr}^2)^{2\nu},$$
$$\lambda_R(T)\propto(T^2-T_{\rm cr}^2)^{\zeta}, \quad x_R(T)\propto(T^2-T_{\rm cr}^2)^{\mu}. \tag{9.6}$$

More precisely, 2β is given by the derivative of $\ln\rho_0(T)$ with respect to $\ln(T_{\rm cr}^2-T^2)$, and similarly for the other parameters. The definition of ζ and μ applies only to the symmetric phase. The exponent $\beta(T)$ is plotted in Fig. 5 along with $x_R(T)$ [the lines marked by (a)] for temperatures approaching $T_{\rm cr}$ for a theory with $\lambda_R=0.2$, $x_R=1$. It is apparent from the temperature dependence of x_R that near $T_{\rm cr}$ the Heisenberg fixed point becomes important. During its evolution the system stays long enough on the critical surface for this fixed point to generate universal critical behavior. The exponent $\beta(T)$ approaches a temperature-independent value

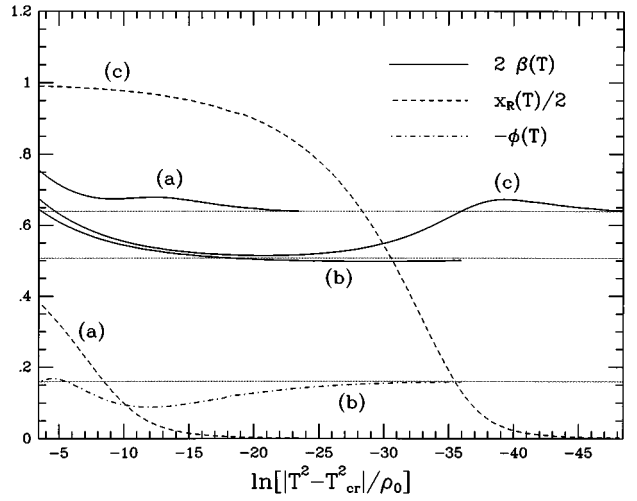

FIG. 5. The critical exponents $\beta(T),\varphi(T)$ and the parameter $x_R(T)$ as the phase transition is approached. The horizontal dotted lines indicate the values of β at the two fixed points and the value of φ at the Cubic fixed point. (a) $\beta(T),x_R(T)$ for a theory with $\lambda_R=0.2$, $x_R=1$. (b) $\beta(T),\varphi(T)$ for a theory with $\lambda_R=0.5$ and x_R slightly smaller than 2. (c) $\beta(T),x_R(T)$ for a theory with $\lambda_R=0.2$, $x_R=1.99$.

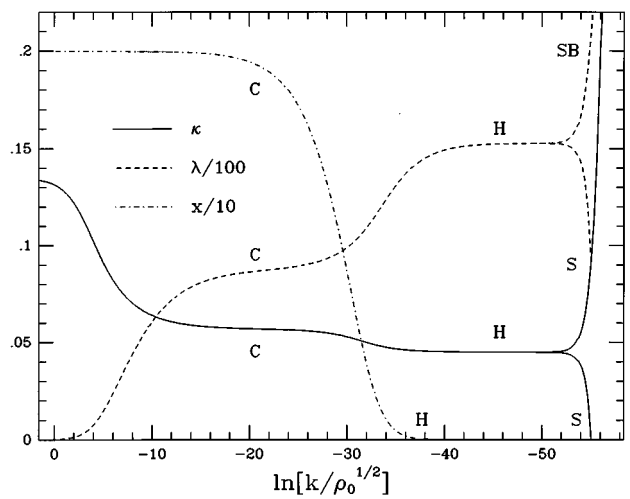

FIG. 6. The evolution of κ, λ, x in the high temperature region, for temperatures slightly above and below the critical one, and $\lambda_R=0.01$, x_R slightly smaller than 2, $T_{cr}^2/\rho_0=3.98$. The system approaches first the cubic and then the Heisenberg fixed point, before deviating towards the symmetric phase or the phase with spontaneous symmetry breaking.

which is independent of λ_R and x_R (as long as $x_R<2$) and characteristic of systems with Heisenberg critical behavior. This value is

$$\beta_H=0.32 \tag{9.7}$$

in agreement with Ref. [6]. Two other exponents are fixed by the scaling laws and the finite value of the ratio $\lambda_R(T)T/m_R(T)$. They are $\nu_H=\zeta_H=2\beta_H$. The above values for the exponents are in rough agreement with known values from three-dimensional field theory [27,38]. The agreement improves dramatically when less restrictive truncations are used for the study of the evolution equation for the potential, and wave-function renormalization effects are taken into account [10]. We have performed this more accurate calculation and obtained results which agree with the known values at the 4–5 % level. This work will be described in Ref. [36]. Finally, the exponent μ also approaches asymptotically a constant value [cf., Eq. (7.5)]

$$\mu_H=\frac{\nu_H}{8\pi^2}\left\{\frac{6}{\kappa_H}[L_1^3(2\lambda_H\kappa_H)-L_1^3(0)] + \lambda_H[9L_2^3(2\lambda_H\kappa_H)+L_2^3(0)]\right\}=0.64. \tag{9.8}$$

X. TRICRITICAL POINT AND CROSSOVER

In the above discussion the Heisenberg fixed point was the only one which played any role. This was expected since the cubic fixed point is repulsive in the x direction. Any flow that starts sufficiently far from it is further repelled and the system never feels its effect. However, it is possible that the values of the running parameters at the beginning of the evolution in the high temperature region are within the reg ion of influence of the cubic fixed point. An example is given in Fig. 6, for a theory with $\lambda_R=0.01$, x_R slightly smaller than 2, and $T_{cr}^2/\rho_0=3.98$. As we have discussed in the introduction and Sec. III, flows that start on the surface $x=2$ in parameter space never move out of it. The flows depicted in Fig. 6 start with $x(T/\theta_2,T)=2-\delta x$ and $\delta x\ll 1$. For this reason, their deviation from the surface $x=2$ is very slow. We display two trajectories which start a small distance $\delta\kappa_{cr}$ above and below the critical surface [and therefore correspond to temperatures slightly below and above the critical one, according to Eq. (8.4)]. For $|\delta\kappa_{cr}|\ll\delta x\ll 1$ the flows stay on the critical surface and close to $x=2$ for a large initial part of the evolution. During this ''time'' they approach the cubic fixed point and stay near it. Finally, $x(k,T)$ starts growing and the system moves away from the repulsive (in the x direction) cubic fixed point and towards the Heisenberg one. After it approaches this attractive (in the x direction) fixed point the evolution is similar to the one depicted in Fig. 3. Systems which start with larger values of $|\delta\kappa_{cr}|$ behave similarly to Fig. 6, but deviate from the critical surface at earlier stages of the evolution. As a result, they can feel the influence of both the cubic and Heisenberg fixed point, or only the cubic one, or they can deviate from the critical surface too soon for any universal behavior to be induced. We calculate the renormalized parameters of the theory (at various temperatures) similarly to the previous subsection. Their behavior as a function of temperature is analogous to that in Fig. 4. The main difference concerns the small region around T_{cr}. In this region the temperature dependence should reflect the influence of the two fixed points during the evolution. We first concentrate on values of $\delta\kappa_{cr}$ for which the critical behavior is dominated by the cubic fixed point. For this region we plot in Fig. 5 the critical exponents corresponding to $\rho_0(T)$ and $x_R(T)$ [lines marked with (b)], which are defined according to

$$\rho_0(T)\propto(T_{cr}^2-T^2)^{2\beta},\quad 2-x_R(T)\propto(T_{cr}^2-T^2)^{-\varphi}. \tag{10.1}$$

We observe that they reach constant values as the critical temperature is approached. The value for β should be characteristic of the cubic fixed point. We find

$$\beta_c=0.25 \tag{10.2}$$

and $\nu_c=\zeta_c=2\beta_c$, in agreement with the scaling laws and the finite value of the ratio $\lambda_R(T)T/m_R(T)$. We expect the cubic fixed point to generate the universal behavior characteristic of an Ising system. This is due to the fact that the theory decomposes into two disconnected Z_2-symmetric theories for $x=2$ (see Introduction and Secs. III and IV). Indeed, the critical exponents that we have calculated are in exact agreement with the results of Ref. [6] for $N=1$, which were obtained at the same level of the truncation scheme. Improved truncations result in values for the exponents which are in agreement with three-dimensional field theory [27,38] at the few percent level [36]. The exponent $\varphi=0.16$ is a typical example of a crossover exponent [25,27]. It is related to the growth of the unstable coupling at the cubic fixed point, and therefore to the negative eigenvalue of the matrix which governs the evolution of small perturbations around the fixed-point value of the parameters.

We postpone a more detailed discussion of the crossover behavior for a future publication [36].

The behavior corresponding to lines (b) of Fig. 5 changes if the critical temperature is further approached (extension of the graph to the right). Eventually the system moves away from the cubic fixed point and the exponents β, ν, ζ take values different from those typical of an Ising system. Also the temperature dependence of $2-x_R(T)$ cannot be described by a crossover exponent anymore and $x_R(T)$ will rather follow Eqs. (9.6), (9.8). We display this behavior in Fig. 5 [lines marked by (c)]. The values of $x_R(T)$ give an indication of which fixed point influences the system. It is clear that the Heisenberg fixed point takes over from the cubic one very close to $T_{\rm cr}$. The temperature dependence of the exponent β is a characteristic example of a crossover curve. It demonstrates how the critical dynamics changes from Ising-like (for $\ln[(T^2-T_{\rm cr}^2)/T_{\rm cr}^2]\simeq -20$) to Heisenberg-like (for $\ln[(T^2-T_{\rm cr}^2)/T_{\rm cr}^2]\simeq -50$). A detailed discussion of this behavior within more accurate truncation schemes will be given in Ref. [36].

XI. FIRST ORDER PHASE TRANSITION

We turn now to the region $x>2$ where we expect a first-order phase transition, as we have explained in Secs. III and VII. Our truncation scheme is too crude to describe the behavior of the potential in this region. We have approximated $U_k(\rho_1,\ \rho_2,\ T)$ by a second-order polynomial in $\rho_{1,2}$. This permits the discussion of potentials with only one minimum. The study of first-order transitions requires the use of improved truncations, where higher ρ derivatives of U_k are taken into account and the possibility of two distinct minima is permitted. This has been done in Ref. [35] for the zero-temperature theory, and the existence of a first-order transition has been established. We shall not repeat this calculation here. Instead we shall derive an explicit solution of the evolution equation in the region of large x, which will demonstrate the existence of first-order transitions for the high-temperature theory.

In Fig. 7 we plot the numerical solution of Eqs. (7.3)–(7.5) in the high-temperature region, for zero-temperature renormalized parameters $\lambda_R=0.01$, $x_R=2.01,3,5$. The temperature is very close to the critical one. We notice that for all three sets of parameters the evolution leads to a region of large x. In Fig. 7 the curves for κ and λ are terminated when $x=30$. We observe that the running parameters tend towards the same area of parameter space. More specifically, for $x=30$ we find (very roughly) $\lambda\sim 3$, $\kappa\sim 0.08$. This convergence of flows was already apparent in Fig. 1. The difference in the evolution lies in the "time" $t=\ln(k/\Lambda)$ that it takes for the various flows to reach the same region. The flows (a) and (b) are fast, while the trajectory (c) starts very close to the surface $x=2$, is first attracted towards the cubic fixed point, and finally deviates towards the region of large x. The cubic fixed point separates the region $x\leqslant 2$, where we have observed second-order phase transitions, from the region $x>2$, for which we expect first-order transitions. For this reason it is characterized as a tricritical point. (The Ising fixed point exhibits similar behavior.)

In the regions of large x we have $\bar{g}\gg\bar{\lambda}$. As a result, the contribution of the ϕ_1 fluctuations to the evolution of

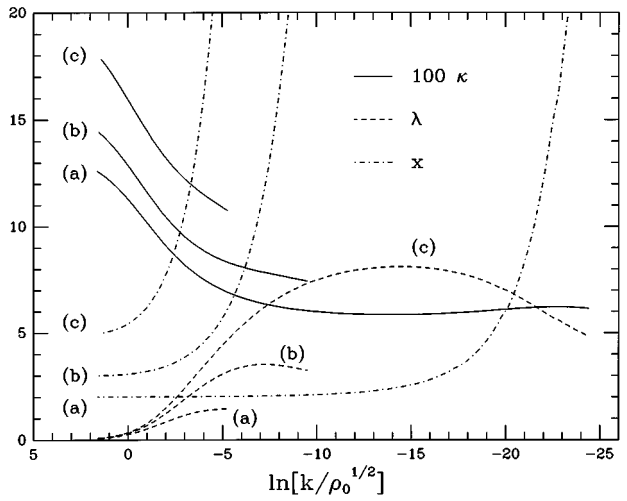

FIG. 7. The evolution of κ, λ, x in the high temperature region for temperatures close to the critical ones. The zero temperature parameters are (a) $\lambda_R=0.2$, $x_R=2.01$, (b) $\lambda_R=0.2$, $x_R=3$, and (c) $\lambda_R=0.2$, $x_R=5$.

$U_k(\rho_1,0,T)$ is suppressed as compared to the contribution of ϕ_2. Moreover, the increase of x in this region is mainly due to the fast decrease of $\bar{\lambda}=\lambda k/T$. In contrast, the coupling $\bar{g}$ evolves only slowly. The ρ_1-dependent mass term for the ϕ_2 field is approximately given by $\bar{g}\rho_1$ (for $\rho_2=0$ and apart from a very small region around the origin) and has again a mild k dependence. Let us assume that for a given scale k_0 the solution of the truncated evolution equations depicted in Fig. 7 gives a good approximation to the exact solution for the potential. (This means, in particular, that a two-minimum structure has not appeared yet at this scale for the true potential.) We denote the parameters of the theory at the scale k_0 by $\kappa_0=\kappa(k_0,T)$, $\bar{\lambda}_0=\bar{\lambda}(k_0,T)$, $\bar{g}_0=\bar{g}(k_0,T)$, $x_0=x(k_0,T)$, and the mass term for the ϕ_2 field by $\bar{g}_0\rho_1$. Based on the remarks at the beginning of this paragraph we can obtain in the high temperature region an approximate solution of the evolution equation (5.3) for the potential on the ρ_1 axis ($\rho_2=0$). By neglecting the first term in the r.h.s. of Eq. (5.3) and the k-dependence of $U_2=\partial U_k/\partial\rho_2$,the differential equation (5.3) is easily integrated. We obtain in the limit $k\to 0$ (up to an irrelevant constant)

$$U(\rho_1,0,T)=U_{k=0}(\rho_1,0,T)$$
$$=\frac{1}{2}\bar{\lambda}_0(\rho_1-\kappa_0 k_0 T)^2$$
$$-\frac{T}{8\pi^2}\int_0^\infty dx\sqrt{x}\,\ln\left[\frac{P_{k0}(x)+\bar{g}_0\rho_1}{x+\bar{g}_0\rho_1}\right]. \tag{11.1}$$

The effective inverse propagator $P(x)$ is given by Eq. (2.11) and we have indicated that it must be evaluated for $k=k_0$. Together with the numerical solution of the flow equations near the critical surface for $k>k_0$, which provides the "integration constants" $\bar{\lambda}_0$, $\bar{g}_0$, and $\kappa_0 k_0 T$, we expect the effective potential of Eq. (11.1) to be a very good approximation. (For a sufficiently small ratio of couplings λ_R/g_R we

may identify k_0 with T/θ_2. This essentially reproduces the results of high-temperature perturbation theory.)

The effective potential of Eq. (11.1) describes indeed a first-order phase transition. This can be most easily visualized if we approximate for the purpose of demonstration

$$P_{k_0}=x \quad \text{for} \quad x>k_0^2,$$
$$P_{k_0}=k_0^2 \quad \text{for} \quad x<k_0^2. \tag{11.2}$$

One finds, for the ρ_1 derivative,

$$U_1(\rho_1,0,T)=\frac{\partial U(\rho_1,0,T)}{\partial\rho_1}$$
$$=-\kappa_0\bar{\lambda}_0 k_0 T+\bar{\lambda}_0\rho_1$$
$$+\frac{\bar{g}_0}{8\pi^2}T\int_0^{k_0^2}dx\sqrt{x}\left(\frac{1}{x+\bar{g}_0\rho_1}-\frac{1}{k_0^2+\bar{g}_0\rho_1}\right). \tag{11.3}$$

Using a rescaled field variable

$$\bar{\rho}=\frac{\bar{g}_0\rho_1}{k_0^2} \tag{11.4}$$

this yields (with $\lambda_0=\bar{\lambda}_0 T/k_0$)

$$U_1(\bar{\rho})=\frac{\bar{g}_0 k_0 T}{4\pi^2}\left[\frac{2}{3}-\frac{4\pi^2\kappa_0}{1+x_0}-\sqrt{\bar{\rho}}\ \arctan\left(\frac{1}{\sqrt{\bar{\rho}}}\right)\right.$$
$$\left.+\frac{4\pi^2}{\lambda_0(1+x_0)^2}\bar{\rho}+\frac{1}{3}\frac{\bar{\rho}}{1+\bar{\rho}}\right]. \tag{11.5}$$

For $\kappa_0<\kappa_A=(1+x_0)/6\pi^2$ the potential $U(\rho_1,\ 0,\ T)$ develops a minimum at the origin ($\rho_1=0$). For κ_0 only slightly below κ_A the origin is only a local minimum whereas the global minimum occurs at $\rho_1\neq 0$ and the model is in the phase with spontaneous symmetry breaking. For sufficiently small κ_0/κ_A, however, the absolute minimum is at the origin and the model is in the symmetric phase. [Note that $\frac{2}{3}-\sqrt{\bar{\rho}}\ \arctan(1/\sqrt{\bar{\rho}})+\frac{1}{3}\bar{\rho}/(1+\bar{\rho})$ is a positive function for all $\bar{\rho}$.] There is a critical ratio κ_0/κ_A [depending on the value of $\lambda_0(1+x_0)^2$] for which the minima at $\rho_1=0$ and $\rho_1\neq 0$ are degenerate in depth, but they are still well separated from each other. Changing κ_0 (which is a function of T) through this critical value leads to a first-order phase transition with a jump in the order parameter.

The necessity of a first-order phase transition can also be seen by considering the ρ_1-dependent quartic coupling $U_{11}(\rho_1)=\partial^2 U(\rho_1,0,T)/\partial\rho_1^2$ which obeys

$$U_{11}(\rho_1)=\bar{\lambda}_0-\frac{\bar{g}_0^2}{8\pi^2}T\int_0^\infty dx\sqrt{x}\left[\frac{1}{(x+\bar{g}_0\rho_1)^2}\right.$$
$$\left.-\frac{1}{[P_{k_0}(x)+\bar{g}_0\rho_1]^2}\right]. \tag{11.6}$$

By keeping only the most singular behavior of the integral for $\rho_1\to 0$ we obtain

$$U_{11}(\rho_1)=\bar{\lambda}_0+\frac{\bar{g}_0^2}{3\pi^2}\frac{T}{k_0}-\frac{\bar{g}_0^{3/2}}{16\pi}T\frac{1}{\sqrt{\rho_1}}. \tag{11.7}$$

We have recovered the leading perturbative result for the behavior of the quartic coupling near a first-order phase transition. If the minimum of the potential $\rho_{10}(k)$ is sufficiently close to zero at the scale k_0, the remaining evolution of $\rho_{10}(k)$ from k_0 to $k=0$ causes U_{11} to vanish at some scale k between 0 and k_0. As a consequence, the minimum at $\rho_{10}\neq 0$ becomes a saddlepoint and disappears subsequently. Already before, a new minimum has been generated at the origin, which remains the only minimum in the subsequent evolution to $k=0$. Since $U_{11}(\rho_1)$ is always negative for sufficiently small ρ_1, the phase transition can never be second order and all values $x>2$ must lead to a first-order phase transition.

Let us finally discuss a suitable choice of the scale k_0 from which on we can replace the numerical solution of the flow equations (7.3)–(7.5) by the approximate solution given by Eq. (11.1). On one hand x_0 must be sufficiently large in order to justify the neglection of the contribution of the ϕ_1 fluctuations in the approximate solution. On the other hand k_0 should be sufficiently high so that a second minimum at the origin has not yet been generated and the truncation of a polynomial around ρ_0 is still valid. This requires that trajectories near the critical trajectory not end at $k=0$ too deeply in the symmetric phase. A realistic choice of k_0 should rather correspond at $k=0$ to the situation where two minima exist simultaneously. For the ''quasicritical'' trajectories depicted in Fig. 7 a reasonable compromise for k_0 seems to be given by the value for which x_0 reaches 30. (This corresponds to $\kappa_A\simeq 0.6$.) The trajectories (a), (b), and (c) shown in Fig. 7 correspond then to potentials $U(\rho_1,\ 0,\ T)$ with two different minima. They are close to, but not equal to, the critical trajectories for which κ would deviate from Fig. 7 towards the end of the running, thus leading to a potential with two degenerate minima.

In summary, we have established the occurrence of a first-order phase transition for $x>2$. Moreover, we have reproduced the perturbative prediction for the form of the potential near the origin. We should emphasize, however, that the perturbative expression applies only to the integration of fluctuations from the scale k_0 (at which $x\gg 1$) to zero. The flow from the region of x near 2 to the region where the perturbative expression becomes valid can be computed only through the use of evolution equations. The different flows correspond to first-order transitions of varying strength. The discontinuity in the expectation value is of the same order as k_0. Also the mass gap at the critical temperature is proportional to this scale. In consequence the discontinuities in ρ for the flows (a), (b), (c) in Fig. 7 have a ratio of $\Delta\rho_a/\Delta\rho_b/\Delta\rho_c=1/0.016/5.1\times 10^{-9}$. The last flow, which remains in the vicinity of the tricritical point before deviating towards the region of large x, corresponds to an extremely weakly-first-order transition.

Our results can easily be extended to the region $x<0$. We have seen in the Introduction and Sec. IV that the AX regime ($x>0$) and the M regime ($x<0$) can be mapped onto each other through a simple redefinition of the fields [in analogy to Eqs. (1.5), (1.6)]. For this reason, the physical behavior in

the two regimes is the same. For example, the cubic and Ising fixed points generate the same universal behavior, characteristic of a Z_2-symmetric scalar theory. Similarly, a first-order phase transition occurs in the region $x<-1$. We shall not repeat our discussion for $x<0$. All our results can be extended to this region by the redefinition of fields and couplings in analogy to Eqs. (1.5), (1.6).

XII. CONCLUSIONS

We have used the formalism of the effective average action for the study of the high temperature phase transition for a theory of two real scalar fields $\chi_{1,2}$, with the symmetry $(\chi_1 \leftrightarrow -\chi_1, \chi_2 \leftrightarrow -\chi_2, \chi_1 \leftrightarrow \chi_2)$, and quartic potential

$$V(\chi_1,\chi_2)=\frac{1}{2}\bar{m}^2(\chi_1^2+\chi_2^2)+\frac{1}{8}\bar{\lambda}(\chi_1^2+\chi_2^2)^2+\frac{1}{4}x\bar{\lambda}\chi_1^2\chi_2^2. \tag{12.1}$$

The phase diagram of the theory is divided into four disconnected regions: $x>2$, $2>x>0$, $0>x>-1$, $x<-1$. Three fixed points with at least one infrared stable direction exist on the surfaces separating these regions: The Heisenberg fixed point ($x=0$) is attractive in the λ and x directions, and corresponds to a theory whose symmetry is increased to O(2). The cubic ($x=2$) and the Ising ($x=-1$) fixed points are attractive in the λ direction and repulsive in the x direction and correspond to two disconnected $Z_2(\chi_{1,2} \leftrightarrow -\chi_{1,2})$-symmetry theories, which are equivalent. The model has a second- or first-order phase transition, with critical temperature well approximated by the perturbative expression if $\bar{\lambda}$ is small.

Theories with classical parameters in the regions $2>x>0$, $0>x>-1$ have a second-order phase transition. Very close to the critical temperature the behavior of the system is universal. It is characterized by critical exponents, which are determined by the Heisenberg fixed point. For theories with classical parameters near the surfaces $x=2$, $x=-1$ the influence of the cubic or Ising fixed point can be observed near—but not too close to—the critical temperature. This leads to a crossover phenomenon, characterized by a crossover exponent and crossover curve, for temperatures approaching T_{cr}. The universal behavior is initially determined by the cubic or Ising fixed point for small enough $(T-T_{cr})/T_{cr}$. As the critical temperature is further approached the more attractive Heisenberg fixed point dominates. No part of this rich structure associated with the second-order phase transition can be observed within perturbation theory. We should mention that for small values of λ the region in temperature where these phenomena appear is rather narrow. This changes for larger λ, where the critical behavior extends over a larger temperature domain without changing the universal results. Even though we concentrated in the present paper on small values of λ for the purpose of comparing with analytical results, our method applies equally well to large λ.

A first-order phase transition is observed in the regions $x>2$, $x<-1$. Therefore, the cubic and Ising fixed points are tricritical points separating regions of second- and first-order transitions. The perturbative expression for the effective potential is a good approximation only for $x \gg 2$ and $x \simeq -2$. All theories near the critical temperature with classical couplings $x>2$ or $x<-1$ correspond to renormalized theories with $x \gg 2$ or $x \simeq -2$ at scales of the order of the mass gap of the model. However, we distinguish two classes of theories.

(I) For classical parameters $x \gg 2$ or $x \simeq -2$ one finds a strongly first-order phase transition. Here the effects of quantum or thermal fluctuations are well approximated by the perturbative expression for the effective potential.

(II) For classical parameters $x \simeq 2$ or $X \simeq -1$ we predict a very weakly-first-order transition. The use of the renormalization group is indispensable for the correct incorporation of the quantum or thermal effects which strongly renormalize the theory towards the regions $x \gg 2$ or $x \simeq -2$.

Our results are relevant for multi-Higgs-scalar extensions of the standard model [22] and multi-scalar models of inflation [23]. They cast doubts on the general validity of perturbative predictions for the high-temperature behavior of these models even in the case of small scalar couplings. High-temperature perturbation theory was found to give a reliable estimate for the effective potential only in limited regions of the parameter space. Our nonperturbative method works for arbitrary values of the couplings in Eq. (12.1) and gives qualitatively reliable predictions for all temperatures and all regions in the phase diagram. Whereas our estimate of the critical temperature can be trusted quantitatively even in the present very rough truncation, some more refined quantities need improved truncations for a precise computation. With the inclusion of χ^6 couplings and anomalous dimension nontrivial quantities such as critical exponents can be calculated with a few percent accuracy [6,10]. Quantitatively more precise predictions for first-order phase transitions can be obtained through the solution of the evolution equation (2.10) for the full effective average potential. Algorithms for the numerical integration of such partial differential equations have been developed recently [39]. The model we have studied is easily extended to the case where χ_1 and χ_2 are N-component vectors with internal SO(N) symmetries. The high-temperature phase transition in other two-scalar models with a different structure of the potential—as for example supersymmetric two-doublet models—can be treated in complete analogy with the present work.

[1] D. A. Kirzhnits and A. D. Linde, Phys. Lett. **42B**, 471 (1972).
[2] L. Dolan and R. Jackiw, Phys. Rev. D **9**, 3320 (1974).
[3] S. Weinberg, Phys. Rev. D **9**, 3357 (1974).
[4] D. A. Kirzhnits and A. D. Linde, Zh. Eksp. Teor. Fiz. **67**, 1263 (1974) [Sov. Phys. JETP **40**, 628 (1974)]; Ann. Phys. (N.Y.) **101**, 195 (1976).
[5] S. Coleman and E. Weinberg, Phys. Rev. D **7**, 1888 (1973); R. Jackiw, *ibid*. **9**, 1686 (1974).
[6] N. Tetradis and C. Wetterich, Nucl. Phys. **B398**, 659 (1993).
[7] C. Wetterich, Nucl. Phys. **B352**, 529 (1991).
[8] C. Wetterich, Z. Phys. C **57**, 451 (1993).
[9] C. Wetterich, Phys. Lett. B **301**, 90 (1993).

[10] N. Tetradis and C. Wetterich, Nucl. Phys. **B422**, 541 (1994).
[11] M. Reuter, N. Tetradis, and C. Wetterich, Nucl. Phys. **B401**, 567 (1993).
[12] N. Tetradis and C. Wetterich, Int. J. Mod. Phys. A **9**, 4029 (1994).
[13] A. Guth and E. Weinberg, Phys. Rev. Lett. **45**, 1131 (1980); E. Witten, Nucl. Phys. **B177**, 477 (1981); A. I. Bochkarev and M. E. Shaposhnikov, Mod. Phys. Lett. A **2**, 417 (1987).
[14] A. D. Linde, Phys. Lett. **96B**, 293 (1980).
[15] M. Reuter and C. Wetterich, Nucl. Phys. **B391**, 147 (1993); **B408**, 91 (1993); **B417**, 181 (1994); **B427**, 291 (1994).
[16] D. Litim, N. Tetradis, and C. Wetterich, Report Nos. HD-THEP-94-23 and OUTP-94-12P (unpublished).
[17] U. Ellwanger and C. Wetterich, Nucl. Phys. **B423**, 137 (1994); M. Reuter and C. Wetterich, Phys. Lett. B **334**, 412 (1994); B. Bergerhoff and C. Wetterich, Nucl. Phys. **B440**, 171 (1995).
[18] V. A. Kuzmin, V. A. Rubakov, and M. E. Shaposhnikov, Phys. Lett. **155B**, 36 (1985); M. E. Shaposhnikov, Nucl. Phys. **B287**, 757 (1987); **B299**, 797 (1988).
[19] L. McLerran, Phys. Rev. Lett. **62**, 1075 (1989); A. I. Bochkarev, S. Y. Khlebnikov, and M. E. Shaposhnikov, Nucl. Phys. **B329**, 493 (1990); A. G. Cohen, D. B. Kaplan, and A. E. Nelson, Phys. Lett. B **245**, 561 (1990); Nucl. Phys. **B349**, 727 (1991); N. Turok and J. Zadrozny, Phys. Rev. Lett. **65**, 2331 (1990); M. Joyce, T. Prokopec, and N. Turok, Phys. Lett. B **338**, 269 (1994); Phys. Rev. Lett. **75**, 1695 (1995); **75**, 3375(E) (1995).
[20] G. W. Anderson and L. J. Hall, Phys. Rev. D **45**, 2685 (1992); M. Carrington, *ibid*. **45**, 2933 (1992); M. Dine, P. Huet, and R. Singleton, Nucl. Phys. **B375**, 625 (1992); M. Dine, R. Leigh, P. Huet, A. Linde, and D. Linde, Phys. Rev. D **46**, 550 (1992); P. Arnold and O. Espinosa, *ibid*. **47**, 3546 (1993); C. G. Boyd, D. E. Brahm, and S. Hsu, *ibid*. **48**, 4963 (1993); J. E. Bagnasco and M. Dine, Phys. Lett. B **303**, 308 (1993); M. Quiros, J. R. Espinosa, and F. Zwirner, *ibid*. **314**, 206 (1993); M. Shaposhnikov, *ibid*. **316**, 112 (1993); P. Arnold and L. Yaffe, Phys. Rev. D **49**, 3003 (1994); W. Buchmuller, Z. Fodor, and A. Hebecker, Phys. Lett. B **331**, 141 (1994); D. Bodeker, W. Buchmuller, Z. Fodor, and T. Helbig, Nucl. Phys. **B423**, 171 (1994); K. Farakos, K. Kajantie, K. Rummukainen, and M. Shaposhnikov, *ibid*. **B425**, 67 (1994); **B442**, 317 (1995); Z. Fodor, J. Hein, K. Jansen, A. Jaster, and I. Montvay, *ibid*. **B439**, 147 (1995); W. Buchmuller and O. Philipsen, *ibid*. **B443**, 47 (1995).
[21] *Electroweak Physics and the Early Universe*, Proceedings of the NATO Advanced Research Workshop, Sintra, Portugal, 1994, edited by J. C. Romas and F. Freire, NATO ASI Series B: Physics, Vol. 338 (Plenum, New York, 1994), and references therein.
[22] A. I.Bochkarev, S. V. Kuzmin, and M. E. Shaposhnikov, Phys. Lett. B **244**, 275 (1990); Phys. Rev. D **43**, 369 (1991); N. Turok and J. Zadrozny, Nucl. Phys. **B369**, 729 (1991); S. Myint, Phys. Lett. B **287**, 325 (1992); J. R. Espinosa, M. Quiros, and F. Zwirner, *ibid*. **307**, 106 (1993).
[23] L. A. Kofman and A. D. Linde, Nucl. Phys. **B282**, 555 (1987); L. A. Kofman and D. Yu. Pogosyan, Phys. Lett. B **214**, 508 (1988); D. S. Salopek, J. R. Bond, and J. M. Bardeen, Phys. Rev. D **40**, 1753 (1989); H. Hodges, G. Blumenthal, L. Kofman, and J. Primack, Nucl. Phys. **B335**, 197 (1990); V. F. Mukhanov and M. I. Zelnikov, Phys. Lett. B **263**, 169 (1991); D. Polarski and A. A. Starobinsky, Nucl. Phys. **B385**, 623 (1992); A. D. Linde, Phys. Rev. D **49**, 748 (1994); A. M. Laycock and A. R. Liddle, *ibid*. **49**, 1827 (1994).
[24] J. Iliopoulos and N. Papanicolaou, Nucl. Phys. **B111**, 209 (1976).
[25] A. Aharony, in *Phase Transitions and Critical Phenomena*, edited by C. Domb and M. S. Greene (Academic, New York, 1976), Vol. VI.
[26] J. Rudnick, Phys. Rev. B **18**, 1406 (1978).
[27] D. J. Amit, *Field Theory, the Renormalization Group, and Critical Phenomena* (World Scientific, Singapore, 1984).
[28] M. Alford and J. March-Russell, Nucl. Phys. **B417**, 527 (1994).
[29] V. Jain and A. Papadopoulos, Phys. Lett. B **314**, 95 (1993).
[30] J. Langer, Ann. Phys. **41**, 108 (1967); **54**, 258 (1969); Physica **73**, 61 (1974).
[31] K. G. Wilson and J. G. Kogut, Phys. Rep. **12**, 75 (1974); F. J. Wegner, in *Phase Transitions and Critical Phenomena* [25]; S. Weinberg, in *Critical Phenomena for Field Theorists*, International School of Subnuclear Physics, Proceedings, Erice, Italy, 1976, edited by Antonio Zichichi (Plenum, New York, 1978); J. Polchinski, Nucl. Phys. **B231**, 269 (1984); A. Hasenfratz and P. Hasenfratz, *ibid*. **B270**, 687 (1986).
[32] T. R. Morris, Phys. Lett. B **334**, 355 (1994).
[33] N. Tetradis and C. Wetterich, Nucl. Phys. **B383**, 197 (1992).
[34] J. Kapusta, *Finite Temperature Field Theory* (Cambridge University Press, Cambridge, England, 1989).
[35] S. Bornholdt, N. Tetradis, and C. Wetterich, Phys. Lett. B **348**, 89 (1995).
[36] P. Büttner, N. Tetradis, and C. Wetterich (in preparation).
[37] W. Buchmüller, Z. Fodor, T. Helbig, and D. Walliser, Ann. Phys. (N.Y.) **234**, 260 (1994).
[38] J. Zinn-Justin, *Quantum Field Theory and Critical Phenomena* (Oxford Science, Oxford, England, 1989).
[39] J. Adams, J. Berges, S. Bornholdt, F. Freire, N. Tetradis, and C. Wetterich, Mod. Phys. Lett. A **10**, 2367 (1995).